24 June 1977, Volume 196, Number 4297 SCIENCE

Neurometrics

Numerical taxonomy identifies different profiles of brain functions within groups of behaviorally similar people.

E. Roy John, B. Z. Karmel, W. C. Corning, P. Easton, D. Brown, H. Ahn, M. John, T. Harmony, L. Prichep, A. Toro, I. Gerson, F. Bartlett, R. Thatcher, H. Kaye, P. Valdes, E. Schwartz

Many data show that brain electrical activity reflects subtle aspects of brain functions including information processing and cognition. Many individuals suffer from disorders of these functions. An unknown but perhaps large percentage of them might benefit from intervention if precise diagnostic information were available. Although current psychological and neurological methods are not sufficiently sensitive for this purpose, electrophysiological measurements of brain functions related to information processing might be of substantial value. However, the acquisition and analysis of electrophysiological data are so complex that evaluation of subtle brain functions by these methods has not become routine.

We have developed a new methodology, called "neurometrics," to provide quantitative information about brain activity related to anatomical integrity, developmental maturation, and mediation of sensory, perceptual, and cognitive processes. The goals of neurometrics are to gather accurate data sensitive to this variety of brain functions, to extract and quantify critical features of these data, and to classify the resulting profiles into clusters sharing common features of brain function by using statistical analysis and numerical taxonomy.

Two related assumptions underlie our approach: first, the EEG (electroencephalogram) and sensory-evoked potentials contain diagnostically valuable information that can be made accessible by quantitative analysis; second, the categories of brain dysfunction revealed by numerical taxonomy of these diagnostic features will represent clusters of individuals with similar electrophysiological profiles of brain function. Each of these subgroups, dissected out of the heterogeneous population who display the same behavioral symptomatology, may have different underlying causes for the similar symptoms and may respond to different treatments.

Computer methods permit quantification of many diagnostically useful features of the EEG, as well as detailed examination of transient electrical oscillations or "evoked potentials" (EP's) elicited by sensory stimuli. Analyses of EP's not only provide information about the structural integrity of the brain, but yield insights into many aspects of brain functions concerned with the reception, encoding, processing, and evaluation of information (*1*, *2*) that are not apparent from visual inspection of the EEG. New capabilities for the quantitative assessment of these more subtle aspects of brain function have important implications for those concerned with cognitive processes, learning, and memory, especially in learning disabled (LD) children and old people with cognitive deterioration.

Although learning disability may be the most common disorder seen by child psychiatrists (*3*), it is often unclear whether a child's learning disability reflects brain dysfunction or is of emotional or environmental origin. Current estimates of the prevalence of LD children range between 7.5 and 15 percent; between 5 and 10 million children in the United States under the age of 15 have some form of brain dysfunction (*4*).

Although psychological methods are better oriented toward the evaluation of cognitive functions than neurological methods, they reflect products rather than processes. Common behavioral manifestations can arise from disparate brain dysfunctions, but lead to similar treatments being used. Behaviorally derived diagnostic schemes are inadequate because of this "functional convergence." Further, some psychometric tests are culture-bound, making it difficult to distinguish between unusual behaviors reflecting different cultural standards. Current diagnostic processes and the subsequent pathological labels are under considerable attack (*5*).

Mathematical techniques from the area known as "numerical taxonomy" permit quantitative neurometric data from many individuals to be used to construct objective, operational classification schemes.

In this article we describe the neurometric procedures devised to achieve the goals listed above and present results obtained from patients with neurological diseases, elderly persons with cognitive impairment, and children with learning disabilities.

Methods

The goals of neurometrics required a new automated, computer-centered technology and a new strategy for diagnosis and remediation of brain dysfunctions. It was necessary to develop: (i) a computer-controlled amplifier system that would reliably acquire data of good technical quality in an optimal format for quantitative analysis; (ii) a standardized set of test conditions (neurometric test

R. John is professor of psychiatry and director of the Brain Research Laboratories of the department of psychiatry, New York University Medical Center; B. Z. Karmel is at the University of Connecticut at Storrs; W. C. Corning is at the University of Waterloo; I. Gerson is at Jefferson Medical College, Philadelphia; H. Kaye is at the State University at Stony Brook, New York; T. Harmony and P. Valdes are at the Centro Nacional de Investigaciones Cientificas de la Universidad de la Habana, Cuba; all other authors are members of the Brain Research Laboratories, New York University.

battery, or NB) constituting appropriate challenges of a wide range of brain functions with probable diagnostic utility that could be presented by a computer-controlled stimulator; (iii) analytic programs to extract quantitative features of the electrophysiological activity recorded under these test conditions; (iv) multivariate statistical procedures to evaluate the probability of all derived measures relative to normative data bases to redefine concepts of "normal" or "abnormal"; (v) easily comprehensible display methods; and (vi) adequate techniques for numerical taxonomy which would utilize all observed features to classify individuals independently of a priori categorization.

A digital electrophysiological data acquisition and analysis system (DEDAAS) was constructed to meet this set of specifications. The DEDAAS uses up to 24 solid state EEG amplifiers (*2*) which have precise fixed gain, low noise, high common-mode rejection ratios, sharp 60-hertz filters to eliminate the need for a shielded room, high-input impedance to reduce the influence of variation in electrode impedance, and freedom from drift.

The output of the amplifiers goes to a PDP 11 computer (11/45, 11/10, or 11/03 microprocessor) that can calibrate the amplifiers or check the electrode impedances automatically. The 10/20 International Electrode System occupies 19 channels, and channel 20 is used to monitor eye movements. Remaining channels permit accelerometer, electrocardiogram, or other recordings. An array of light-emitting diodes, one corresponding to each electrode position in the 10/20 system, plus an oscilloscope, permits visual monitoring of local EEG events and pinpoints channels with unacceptable recording characteristics.

Simultaneous monopolar recordings are obtained of the full 10/20 system referenced to linked earlobes. These analog data are transformed by an analog-to-digital converter and stored on digital tape, disk, or cassette. Conventional bipolar montages or any desired compound electrode can be constructed subsequently by computer simulation. Routinely, we compute 57 electrode combinations or derivations (19 monopolar, 19 coronal bipolar, and 19 sagittal bipolar pairs). Frequency and voltage limits specified for every channel are constantly monitored, permitting the computer automatically to reject data contaminated by eye or body movement, or by high electrode impedance. One option accepts but marks all data considered questionable; another option rejects such data. *We routinely edit these data prior to quantitative analysis, examining conventional records reconstructed from the digital data to reassure ourselves of the adequacy of artifact rejection*, which is fairly satisfactory. The DEDAAS routinely yields usable data from newborn infants, hyperactive children, and restless geriatric patients who would normally be extremely difficult or impossible to examine; DEDAAS simply waits until artifact-free segments of data occur, combining these into a sample sufficiently large for adequate analysis.

Required stimulus sequences are presented automatically with the use of the computer-controlled stimulator and the NB program. Complete stimulation protocols are incorporated into the digital record to permit subsequent automatic data analysis without operator intervention.

The initial version of the NB and the analysis procedures was constructed on the basis of our personal experience and judgment as to what test conditions would best reveal behaviorally significant dysfunctions and what features extracted from such data would be of critical diagnostic utility. We were especially influenced by certain previous findings which are summarized below.

Analysis of the EEG in Neuropathology

Normative baselines are available for the frequency composition of the EEG from birth to maturity (*6*), and for the symmetry of EEG waveshape and amplitude between bilaterally symmetrical, or homologous, derivations (*7*). These permit quantification of maturational lag from the spectral composition of the EEG. Not only many types of neuropathology but also learning and performance difficulties are often correlated with excessive slow-wave activity and EEG asymmetries (*8, 9*).

Quantitative frequency analysis reveals various kinds of neuropathology (*10*). Matoušek and Petersén (*11*) compared the ratio of power in the delta plus theta frequency bands (1.5 to 7.0 hertz) in the average normal adult to that of neurological patients, separately for each different head region. Values below 0.8 were considered abnormal, indicative of excessive slow waves. This "age-dependent quotient" (so called because age-specific normal values were used) was then plotted to show the distribution of excessive slow waves on the head. The region with the greatest excess was considered the probable locus of the pathological process. The locations of brain tumors were accurately determined by this method.

A different strategy is based on the assumption that many kinds of neuropathology involve a unilateral disruption of brain function and might therefore decrease electrical symmetry. Otero *et al.* (*9*) and Ricardo *et al.* (*12*) used a special-purpose symmetry analyzer to quantify the similarity of waveshape and amplitude of EEG signals from symmetrical pairs of electrodes in a large sample of neurological patients with confirmed lesions. Discriminant analysis separated tumor (87 percent) and stroke (80 percent) patients from normals with an accuracy comparable to current results obtained with conventional EEG (*13*), but was of little use for the detection of epilepsy. These workers then used multiple discriminant analysis as a type of numerical taxonomy (*14*). Although tumor and stroke detection rates remained high and substantial differential diagnosis could be made, false positives increased to an undesirable level.

Analysis of Average Evoked Response Symmetry in Neuropathology

The evoked potential (EP), a transient electrical oscillation representing the response of a brain region to sensory stimulation, is frequently obscured by ongoing EEG activity. By computer averaging, the waveshape of an averaged evoked response (AER) can be extracted from EEG activity. This waveshape reflects the spatial and temporal characteristics of the responding neural systems, and is a sensitive indicator of sensory, perceptual, and cognitive processes, or the presence of neuropathology.

It is difficult to decide whether any individual AER waveshape differs significantly from a "normal" contour. The problem of defining a "normal" waveshape can be partially circumvented by evaluation of the asymmetry of AER's simultaneously computed from homologous derivations, which also reduces concern about variations between individuals.

Normative data are available for average correlation coefficients, peak amplitude discrepancies, peak latency discrepancies, and signal energy ratios between AER's, from 16 derivations recorded in each of 144 normal healthy young adults (*15*). These data reveal extremely high AER waveshape symmetry.

Although moderate amplitude asymmetry is correlated with normal lateralization of function (*16*), extreme amplitude asymmetry is a sign of pathology. Asymmetry of the AER is a sensitive index of brain dysfunction, often appearing in patients without subjective complaints and with negative neurological and EEG findings in whom neuropathology is subsequently confirmed by other methods. Qualitative assessment of symmetry was reported to give accurate (90 percent) detection of tumors and cerebrovascular accidents (*17*). Otero *et al.* (*14*) obtained quantitative AER symmetry measures on 177 patients with various neurological diseases. A discriminant function between these patients and a group of 144 normal subjects yielded detection accuracies of 82 percent for tumors, 82 percent for strokes, 63 percent for epilepsy, and 74 percent for miscellaneous neurological diseases.

Harmony (*18*) compared the accuracy of discriminant functions based upon EEG or AER symmetry with conventional EEG evaluation, using 150 neurological patients for which all three kinds of data were available (Table 1). Numerical methods were superior to visual evaluation of the EEG, except in the case of epilepsy. When computer assessment was combined with the conventional EEG, overall accuracy increased to over 94 percent. These results suggest the practical clinical utility of these methods, not only for rapid evaluation by paramedical personnel of patients at risk for brain disease, but as an adjunct to the conventional EEG. However, these methods are as yet of little utility for differential diagnosis between different neurological diseases.

Table 1. Relative overall accuracy of EEG symmetry, AER symmetry, and conventional EEG for each disease category (*18*).

Disease category	Positive cases found					
	EEG symmetry		AER symmetry		EEG	
	N	Percent	*N*	Percent	*N*	Percent
Tumors	26	84	22	71	22	71
Strokes	46	87	42	79	32	60
Epilepsy	29	73	23	58	33	83
Miscellaneous	18	69	20	77	17	65
Total	119	79	107	71	104	69

The Average Evoked Response Related to Sensation, Perception, and Cognition

Sensory acuity. The AER can be used to estimate auditory thresholds and to assess the sharpness of retinal imaging (*19*). To obviate the limitations imposed by visual examination, we constructed a special-purpose computer to assess the significance of the difference between two AER's, utilizing the corresponding variances to compute the *t*-test at each point along the analysis epoch (*20*). This method permits comparison of the symmetry of two AER's simultaneously computed from homologous regions or sequentially computed from the same region to assess differences between responses to different stimulus conditions. If one condition is the absence and the other is the presence of stimuli of specifiable intensity, estimates of sensory thresholds can be obtained.

This method was used to construct a screening test of visual acuity. When a fine spatial grid is replaced by a coarse grid so that contrast is perceived in a previously homogeneous visual field, a marked change occurs in the AER at a latency of about 150 milliseconds (*1, 21*). Comparisons made with the *t*-test of AER's recorded under these two conditions show a significant difference at that latency if the subject can perceive the difference between the stimuli. Finer gradations of the spatial grid can permit more accurate acuity estimates. An analogous procedure may be useful for evoked response audiometry (*19*).

Perceptual capabilities. Aberrant AER features related to perceptual dysfunction have been reported for persons with psychiatric disorders (*22*), and one explanation of schizophrenic symptomatology points to perceptual dysfunction as a critical predisposing factor (*23*). The AER is sensitive to perceptual as well as sensory processes: for example, different AER's are obtained with two different colors except in the color-blind person (*24*) or with two different geometric shapes equated for size (*25, 26*). Screening tests for perceptual dysfunctions have often been and certainly should be a standard part of clinical evaluations. We have devised such tests using a *t*-test strategy analogous to the one described above for sensory acuity (*20*).

Cognitive processes. It is difficult to identify cognitive disorders, especially in children, when the tests used are verbal and culture-bound, measuring product without describing process. Electrophysiological techniques may circumvent these limitations, yielding more direct insight into brain mechanisms mediating basic cognitive processes.

1) Changes in the AER with age might serve as measures of maturation and of postconceptional age (*27*), and may be relevant for the assessment of cognitive function. The waveshapes obtained from mentally retarded children are smaller and less complex than in normal children. Asymmetry of evoked and spontaneous activity in anterior temporal regions, involved in language function, appears with maturation and may reflect lateralization of neural processes related to language acquisition (*28*). Other findings suggest hemispheric lateralization of responses to signals representing primarily verbal or spatial concepts (*29*). Finally, the waveshape elicited by a visual form of specified shape contains features independent of size (*25*). These invariant features may reflect a physiological concomitant of abstraction; a square is a square regardless of its size. This perceptual constancy cannot be innate, but must be acquired by maturation and experience, as an individual constructs generalizations from idiosyncratic experiences.

2) The capacity to control afferent input is a universal adaptive property of brains. The AER method can be used to reveal: (i) "habituation," or the diminution of responses to repetitious inconsequential events (*30*); and (ii) "selective attention," or the enhancing of salient features of the environment (figure) with the suppression of inconsequential aspects (ground) when two differentially relevant events occur within the same (*31*) or different (*32*) modalities. Children with learning disability or other brain dysfunctions are frequently incapable of structuring adaptive figure-ground relations (*33*). The inability to habituate the AER may be an early indicator of disorder (*34*).

3) The extraction of invariant features from different stimuli with the same meaning can be assessed by the AER. Certain features of the AER remain constant when geometric forms of the same shape but different sizes (*25*), large and small versions of the same letter of the alphabet (*35*), or the same word printed in upper or lower case letters are presented to the subject (*36*).

4) Short-term memory and expec-

tancies based upon systematic relationships between environmental events are reflected by the AER. A late positive component (latency about 300 msec; $P_{\overline{300}}$) reflects the effect of a match or mismatch between predictions and actual events (*37, 38*). When the actual event can be predicted, $P_{\overline{300}}$ is suppressed or absent. The brain seems to use a representation of recent experience to generate expectations about future events. Match-mismatch operations are involved in the response to novelty, focusing attention, habituation, and the organization of memory, as well as in cognitive processes involved in comparisons of word meaning. These processes are reflected in late positive components of the AER (*38*). The AER also seems to reflect memory readout processes: "emitted" AER's appear in human subjects at the time of expected but absent events (*39, 40*).

5) In cats, AER waveshapes elicited by neutral stimuli in differential generalization tests are not determined by the actual stimulus but correspond to the waveshape usually elicited by the appropriate cue for the behavior subsequently performed (*41, 42*). Experiments with humans similarly demonstrate that the AER waveshape can be decisively influenced by the conceptual set of the subject, or by the interpretation of an ambiguous event. For example, AER's elicited in a task monitoring single or double clicks which might be loud or soft displayed two components if the instructed set was for multiplicity, but only one component if the instructed set was for intensity (*39*). Different AER waveshapes are elicited when the same spoken (*43*) or printed (*36*) word is embedded in syntactical context as a verb or a noun. We have found an anatomical differentiation between processes reflecting exogenous sensory input and endogenous memory readout (*35*). When the same visual stimulus was interpreted as a letter or as a number, AER's from parietal regions reflected these differences while AER's from occipital regions remained unchanged. Conversely, when two different visual stimuli with the same meaning were presented, occipital AER's reflected the physical differences while parietal AER's reflected their identical meaning. Analogous results have been reported by others (*44*).

6) The waveshape of the AER elicited by a novel stimulus changes as it becomes established as a conditioned stimulus (*41, 45*). Since very young infants can be conditioned with corresponding AER changes (*46*), it is now possible to evaluate associative learning capacity within and between sensory modalities and different brain regions throughout the developmental span.

7) Finally, AER measures have already been demonstrated to correlate with various behavioral disorders (*2*). For example, differences in amplitudes of late components of the AER occur between good and poor readers, and read-

Table 2. Present content of the neurometric test battery with a brief indication of the intended purpose of each item.

Neurometric test item	Intended purpose
EEG conditions and challenges	
1. Eyes open, spontaneous EEG	Baseline measures
2. Eyes closed, resting EEG	Yields age-dependent quotient
3. Eyes open minus eyes closed	Effect of removal of visual input
4. Photic driving at 2.5, 5, 10, and 18 hertz	Yields reactivity in delta, theta, alpha, and beta ranges when compared with baseline measures
AER conditions and challenges	
Sensory acuity	
5. 65 lines per inch, 50 percent transmission	Perceived as a blank flash
6. 27 lines per inch, 50 percent transmission	Seen as checkerboard if visual acuity is approximately 20/20
7. 7 lines per inch, 50 percent transmission	Seen as checkerboard unless visual acuity is worse than 20/200
8. 45 db click	Elicits auditory AER unless hearing loss is sufficiently severe to interfere with language acquisition
Pattern perception	
9. Large square	Each contributes to an estimate of perception of differences in geometric forms but preservation of shape invariance independent of size
10. Small square	
11. Large diamond	
12. Small diamond	
13. "b"	Each contributes to estimates of central discrimination between shapes of letters most commonly reversed
14. "d"	
15. "p"	
16. "q"	
Prediction of temporal order	
17. Random versus regular flash	Change in AER waveshape reflects diminished response to predictable stimuli, indicates recognition of repeated temporal sequence
18. Random versus regular click	
19. Random versus regular tap	
20. Phasic habituation	Reveals rate and amount of suppression of information input about a meaningless monotonous event, reflects attention and short-term memory
21. Dishabituation	Indicates whether suppressed input is nonetheless continuously monitored to permit detection of possible change
22. Rehabituation	By comparison with initial phasic habituation, reveals whether suppression of meaningless input is facilitated by memory of previous experience
Sensory-sensory interactions	
23–25. Passive interactions between visual, auditory, and somatosensory systems	Reveals increase or decrease in response of brain as a result of simultaneous presentation of simple stimuli in different sensory modalities
26. Flash followed by click 250 msec later	Measure of recovery cycle after visual input
27. Click followed by flash 250 msec later	Measure of recovery cycle after auditory input

ing disabled children have smaller component amplitudes at $P_{\overline{300}}$ (*47*), hyperactive children have small amplitude $P_{\overline{200}}$ and large amplitude $N_{\overline{250}}$ components (*48*); various deviations from usual AER waveshapes have been found in children with learning disabilities (*49*); changes in AER features appear in severely retarded children (*34, 50*), and characteristics of the AER may predict the outcome of certain pharmacotherapeutic interventions (*51*).

The Neurometric Test Battery and the Measure Set

The neurometric test battery (NB), which is based upon the research findings reviewed above, does not require verbal interaction nor overt behavioral response, and thus substantially circumvents the developmental, linguistic, and cultural limitations of psychometric tests. The NB yields EEG and EP data from a sequence of conditions and comparisons between related conditions which are termed "challenges" and are comparable to test items (Table 2). A computer-controlled stimulator contains a photo-flash tube, a source of oscillating light, an automatic slide projector, click and pure tone (250, 500, 1000, and 3000 hertz) sources of specified intensity, and a tactile stimulator. A video set and a cassette player provide other visual and auditory stimuli.

From the data recorded for each electrode derivation under every NB condition and challenge, a variety of numerical features are extracted.

EEG features. Under each EEG condition, 12 samples of "artifact-free" EEG's are recorded, each of 5 seconds. After being visually edited to further rule out artifacts, numerical features for each derivation are computed from each sample separately and mean values and standard deviations are calculated for the full set of samples. These indices, in hertz, are: (i) absolute power in low delta (0.5 to 1.5), high delta (1.5 to 3.5), alpha (7 to 13), low beta (13 to 19), high beta (19 to 25), gamma (25 to 40), and total (0.5 to 40) frequency bands; (ii) relative power (percentage) in each frequency band; (iii) ratio of delta plus theta to alpha power; (iv) power symmetry within each frequency band between each pair of symmetrical (homologous) derivations; and (v) waveshape symmetry as assessed by cross-correlation of the total signals and by coherence within each frequency band between each homologous pair. These computations yield quantitative estimates of 1272 indices under every EEG condition and challenge.

AER features. Under each AER condition, the AER of every derivation is computed from 64 evoked potentials yielding the digitized average signal voltage and its variance at each of 100 time

Table 2 (continued).

Neurometric test item	Intended purpose
Figure-ground relations	
28–30. Interaction between meaningful visual input (figure, consisting of scenes on a video screen) and meaningless visual, auditory, or somatosensory input (ground)	Reflects dynamic structuring of figure-ground relationships which require discrimination between relevant visual "signal" and irrelevant "noise," which may be either ipsimodal (video-visual) or cross-modal (video-auditory or video-somatosensory)
31–33. Interaction between meaningful auditory input (figure, consisting of a tape recording of a musical selection or story) and meaningless visual, auditory, or somatosensory input (ground)	Reflects dynamic structuring of figure-ground relationships requiring discrimination between relevant auditory "signal" and irrelevant "noise," which may be either ipsimodal (music-auditory) or cross-modal (music-visual or music-somatosensory)
Conditioned response evaluation	
34. Visual stimulus, before conditioning	Baseline control measures
35. Auditory stimulus, before conditioning	Baseline control measures
36. Somatosensory stimulus, before conditioning	Baseline control measures
After sensory-sensory conditioning with visual conditioned stimulus and auditory unconditioned stimulus:	
37. Visual stimulus	Reflects effects of conditioning as specific changes in response to conditioned stimulus
38. Auditory stimulus	Control for "sensitization," revealed as generalized change to unconditioned as well as conditioned stimulus
39. Somatosensory stimulus	Control for "pseudoconditioning," revealed as generalized change to any stimulus
After sensory-sensory conditioning with auditory conditioned stimulus and visual unconditioned stimulus	
40. Visual stimulus	Control for sensitization
41. Auditory stimulus	Estimate of specific conditioning effect
42. Somatosensory stimulus	Control for pseudoconditioning
EEG conditions and challenges	
43. Eyes open, spontaneous EEG	Replication of initial measures
44. Eyes closed, resting EEG	
45. Eyes open minus eyes closed	
46. Eyes open, beginning, minus eyes open, end	Estimate of effects due to state, such as anxiety about test or fatigue due to testing, versus characteristic individual features displayed across states
47. Eyes closed, beginning, minus eyes closed, end	

points, sampled at 10-msec intervals across a 1-second analysis epoch. A number of additional indices are extracted from these data which reflect critical features of the response. These derived features are computed for the whole analysis epoch and for each of four latency intervals corresponding to components or waveshape segments of special interest. The computed features are: (i) signal power; (ii) variance, or "noise"; (iii) signal-to-noise ratio; (iv) mean squared first difference, which is proportional to the product of the signal power and mean squared signal frequency; (v) difference in signal energy between homologous pairs; (vi) normalized difference in signal power between homologous pairs, broken down into one term representing power asymmetry and one term representing waveshape asymmetry; (vii) cross-correlation coefficient [for details, see (*2*)]. Programs are being tested which are intended to provide: (viii) peak amplitude for each of eight components; (ix) peak latency for the same components; (x) peak amplitude asymmetry, both absolute and relative, for each component; and (xi) latency lag, for each component. These computations yield about 2000 derived indices, plus 5700 AER and variance values, for each AER condition and challenge.

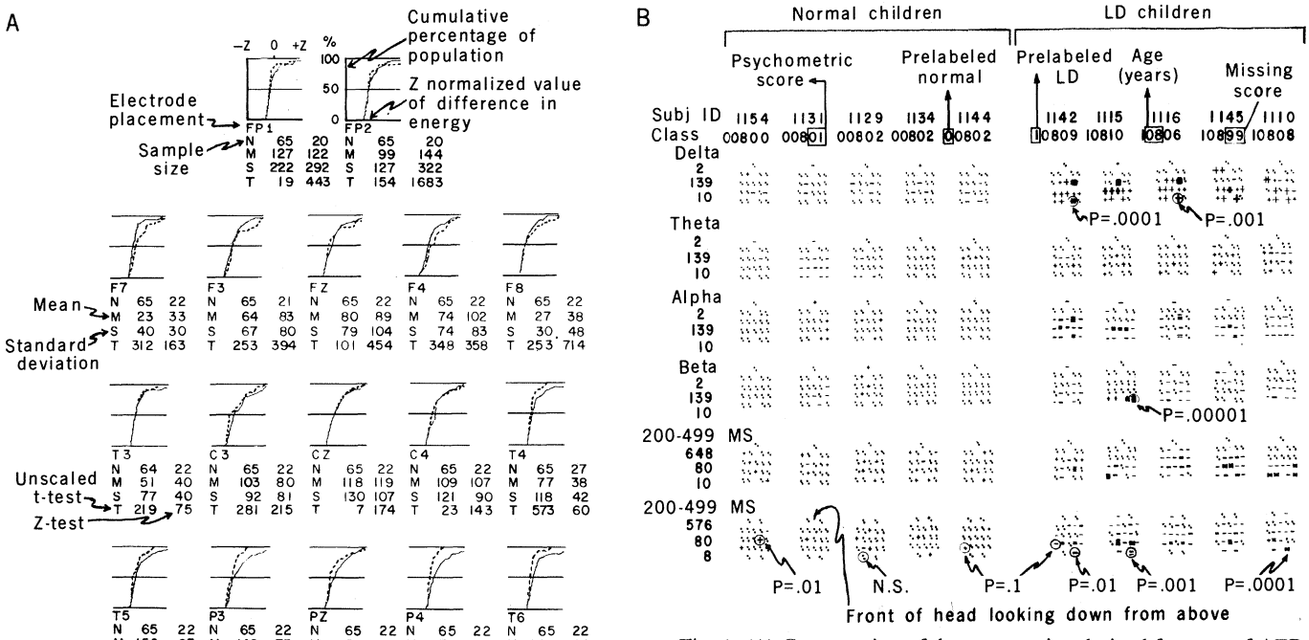

Fig. 1. (A) Compression of data comparing derived features of AER waveshapes recorded from 19 electrode placements of the 10/20 system in a sample of 65 normal and 22 LD children. The overall display represents the topography of the electrode array viewed from above, with the front of the head oriented toward the top of the display. Each graph compares the cumulative histograms for two different groups of subjects, for selected NB parameters or a combination of parameters recorded at the corresponding electrode position. This example shows the distribution of the Z transform of the difference in the 200- to 500-msec latency domain (P_{300}) in the power of AER's elicited by random and regular light flashes. At electrodes P_3, P_4, and T_6, the LD group shows a significantly *smaller* AER difference between these two stimulus conditions than the normal group ($P < .001$). This finding suggests that some LD children do not use orderly environmental relations to make predictions about future events in the same way as normal children, since the energy of P_{300} is known to reflect the amount of uncertainty about an event (*37, 38*). (B) Illustrative density coded Z-transformed displays of neurometric indices extracted from various EEG and AER conditions of the NB. Each column of displays represents data obtained from one subject, while each row represents one univariate or multivariate index. Each display represents an array of entries: each entry corresponds to the value of the index measured at that point on the subject's head, while the position of the entries in the array corresponds to the electrode locations of the 10/20 system. For each index, the entry at any location has been density coded to reflect the Z transformation of the measure obtained from that subject referred to the mean of the whole population. If the Z-transformed value was such that the P level of obtaining that value by chance was not less than .1, two small spots (·.) were entered to convey that the measure was assessed and found within the normal range. If the value of Z was such that the P level was between .1 and .01, a small + was entered to show that the index was unusually large or a small − was entered if the index was unusually small; if the P level was between .01 and .001, a large + was entered if the value was abnormally high or a large − if it was abnormally low; if the P level was between .001 and .0001, a double ++ or = was entered; between .0001 and .00001, a triple +++ or ≡ was entered; P levels below .00001 were indicated by large solid shapes in the form of + or − signs. The data are for five normal and five LD children selected from a much larger sample and are to be considered as illustrative examples rather than as invariable findings. The displays in rows 1 to 4 show the distribution of relative power (code 139) in the spontaneous EEG, recorded from bipolar derivations (code 10) with eyes closed (code 2), respectively from top down in the delta, theta, alpha, and beta bands. Note the typical excess of slow delta activity predominantly in posterior head regions of the LD subjects, usually coupled with a deficiency of alpha and sometimes of beta activity. In row 5 the LD subjects show significantly less change in the signal energy (code 80) of the bipolar (code 10) AER in the latency region between 200 and 499 msec when a flash is delivered randomly while the subject is watching a TV cartoon than when a flash is delivered randomly while the subject looks at the defocused TV screen (code 648). Row 6 shows that the LD subjects display significantly less change in the signal energy (code 80) of the monopolar (code 8) AER in the latency region between 200 and 500 msec when a random is compared with a regular flash (code 576). The particular head regions displaying this less-than-expected difference when the two conditions are compared vary from subject to subject. Such findings suggest, however, that LD children tend to display less suppression at P_{300} to an irrelevant stimulus (ground) in the presence of meaningful environmental input (figure) and, analogously, display less of a tendency to distinguish between predictable and unpredictable events in the environment. This is reflected in the similarity of late positive components in AER's elicited by these two different kinds of events, and supports the observations in (A).

Evaluation and Display Techniques

The digitized AER waveshape can be represented as a signal vector in a 100-dimensional time space, where each dimension corresponds to the signal voltage at a different latency point in the analysis epoch. Principal component analysis can identify the actual dimensionality of the "signal space" containing a set of such vectors representing AER's from many derivations in the same individual or from the same derivations in many individuals (*52*). One can now construct a parsimonious description of each AER as a linear combination of a set of terms. Each term defines the relative contribution ("weighting," whose square is proportional to the percentage of signal power) of each basic dimension (factor) to that AER. These linear equations enable great data compression, since any AER in that signal space can be described as some combination of the same basic factors. Thus, patterns of factor weightings can be used to construct clusters of AER's with distinctive morphology.

Compression, evaluation, and display techniques were required to make the huge volume of available NB data comprehensible. As the first step, baseline data were obtained for all or part of the NB from groups of healthy individuals in several age ranges of interest: newborn infants, elementary school children, and elderly adults. Group means and standard deviations were computed for every quantitative index. This made it possible to use the *t*-test to compare subgroups on any condition or to compare conditions within any subgroup. Comprehension of differences between subgroups can be facilitated by appropriate displays, such as POPHIS, shown in Fig. 1A. This display superimposes cumulative distributions of original or *Z*-transformed indices for two subgroups upon 19 graphs. Each graph represents a different electrode derivation and is located in the display relative to the position of that derivation on the head. These graphs can describe distributions of uni- or multivariate indices, differences between conditions which define challenges, or differences between bilaterally symmetrical locations. Below each graph, data about sample size, mean values, standard deviations, and *t*- and *Z*-tests further document the observed differences.

The Z Vector

Evaluation of the data from any individual is based on a procedure that is the most powerful strategy of neurometrics. Each NB index is subjected to *Z* transformation, such that the difference between the individual index and the group mean value is divided by the standard deviation of the whole sample. This has four major consequences: (i) the individual index is transformed from its original units to a metric reflecting the *relative probability* of that value within a healthy normal reference group. "Abnormality" is defined statistically as improbable values exceeding those expected randomly, allowing for the large size of the measure set. It is especially useful to display the anatomical location of all improbable indices found within any individual. Existing knowledge about the functional role of different cortical regions, together with the presumed processes probed by each NB item, provide the basis for tentative prediction of the possible behavioral implications of the individual profile of improbable values (*53*). In such displays (Fig. 1B), a localized region on a head diagram represents the position of each derivation. The *density* of shading in each local domain is proportional to deviations from the normative reference in positive (+ entries) or negative (− entries) directions. This rapid overview of the findings in any individual provides a visual indication of the severity, type, and anatomical locus of abnormality, analogous to a "functional electrophysiological brain scan"; (ii) indices describing disparate dimensions, such as voltage, time, latency, coherence, and symmetry are transformed to the common metric of probability. It therefore becomes possible to compare or combine measures that were initially not dimensionally comparable; (iii) most important, the abnormality profile of any individual can now be represented as a **Z** vector (or **Z**) in an NB-dimensional probability space. The **Z** of the perfectly normal individual only randomly leaves the *normal domain* defined by a hypercube with side = $2Z = 2 \times 1.96$ ($P \leq .05$ on each dimension independently) centered at the origin of this space; and (iv) the distance matrix, D_{ij}, can now be computed between **Z** representing each individual and **Z** of every other relevant individual, yielding interindividual distances in probabilistic terms.

The more unusual any NB index in an individual, the greater the component of **Z** in the corresponding dimension. Thus, the overall *length* of **Z** provides the quantitative and objective criterion for the *severity* of brain dysfunction in an individual. From this viewpoint, the distinction between "normality" and "abnormality" depends upon the threshold value established in any particular set of dimensions. The multivariate *nature* of the dysfunction is defined by the *orientation* of **Z**. Thus, **Z** provides the basis for an objective diagnostic classification scheme, as well as a way to compensate for the large number of false-positive findings to be expected by chance, given the large size of the set of NB indices.

For all NB indices, the probabilities of a random positive finding are roughly equal. Given a population of normal healthy subjects, one would expect the **Z** vectors representing such random hits to be randomly distributed throughout the NB-dimensional probability space. Using the distance matrix computation, one can determine the actual density of **Z** points in any domain of this space and compare it to the density reasonably expected by chance. Regions of high density reflect the improbable similarity of profiles of improbable values shared by a group, or cluster, of individuals. Presumably, these individuals share a similar set of brain dysfunctions; they constitute a potential diagnostic category. Membership in a particular cluster thus suggests a common etiology for the observed pattern of dysfunction and potentially provides a basis for the rational selection of differential treatment.

Although **Z** is here discussed only in the context of brain dysfunction, this concept can be generalized to problems in other fields, and may provide the basis for a numerical taxonomic approach to other areas of medical diagnosis.

Classification Strategies Based on Numerical Taxonomy

Numerical taxonomy refers to techniques intended to identify groupings of data points in multidimensional spaces. If the measure set contains relevant variables, objectively evaluated and spanning a substantial dimensionality, members of clusters will share functional characteristics. Clusters will be more related to natural structure within the population than to any a priori bias. Numerical taxonomic methods have been used in the classification of schizophrenics (*54*), so-called "MBD" (minimal brain dysfunction) children (*55*) and AER's (*56*). Some laboratories have used factor analysis to reduce the measure set and have then clustered subjects according to factor loadings (*57*). We have used factor analysis itself as a numerical taxonomic method as well as other techniques.

Factor analysis. Principal component analysis can describe a large set of AER

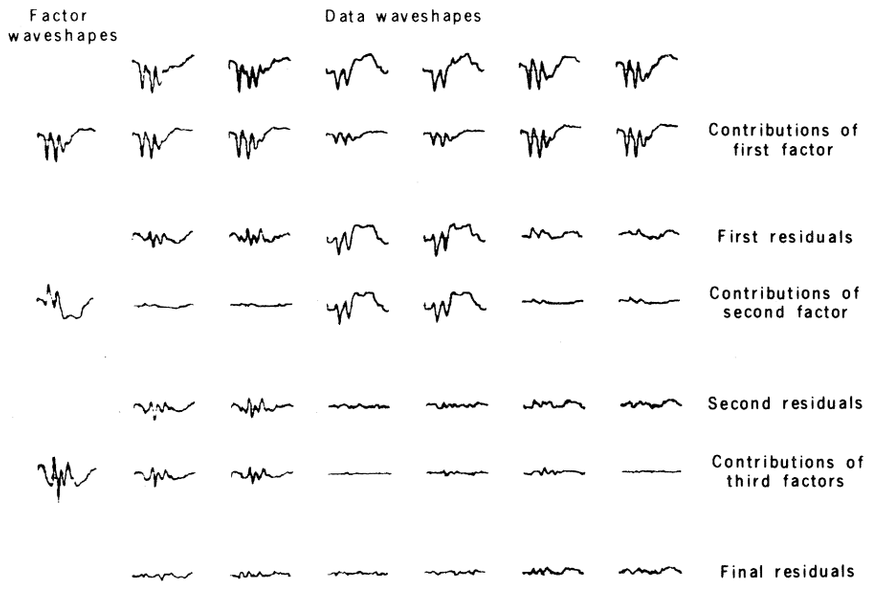

Fig. 2. Factor analysis of a set of AER's. The factor waveshapes in the left column were selected by the varimax procedure and must be regarded as an arbitrary, convenient choice rather than as in any way unique. The justification for this procedure is utility and parsimony. These waveshapes do not necessarily correspond to any real physiological process.

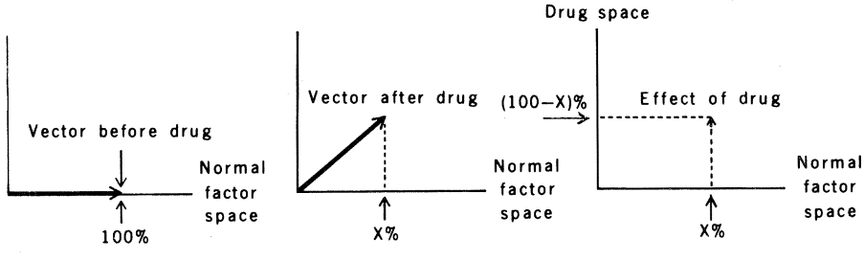

Fig. 3. A residual subspace created by a particular drug, as determined by stepwise factor analysis. Note that the components of the vector in each space have been here described in percentages rather than weighting coefficients.

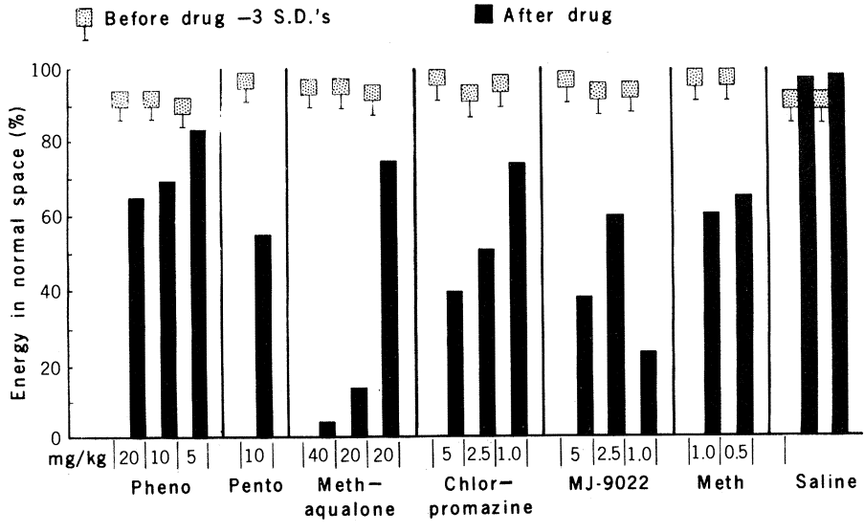

Fig. 4. The percentage of energy in the normal factor space of the visual cortex of a cat that was given different doses of various drugs. The stippled squares represent the percentage of the energy of the average visual evoked potential accounted for by the normal factors before the drug was administered, and the bracket extends three standard deviations below that value. The black bars represent the amount of energy in the response after drug administration which can be accounted for by the normal factors. Drug doses were administered intramuscularly at 1-week intervals, according to a Latin square design. *Pheno*, phenobarbital; *Pento*, pentobarbital; *MJ-9022*, buspirone; *Meth*, methamphetamine.

waveshapes precisely in terms of a small number of quantitative descriptors (*52*). These descriptors, or factors, can be conceptualized as basic waveforms produced by hypothetical signal generators which, mixed in the correct proportions, would reproduce the various AER waveshapes in the set. The first step is to define these factor waveforms as mathematical functions. The second step is to determine the relative contribution, or weighting coefficient, of each factor to every AER waveshape, that is, that coefficient which achieves the best fit between the waveform of that factor and the AER waveshape. Each AER waveshape in the set can be described as the linear sum of each factor multiplied by the weighting representing its relative contribution to that AER waveshape. Precise comparisons between the individual members of a set of AER waveshapes can thus be reduced to comparison of the relative weights of corresponding factors, since the mathematical function describing any factor remains unchanged no matter how much it contributes to any AER.

The set of all waveshapes that can be described by a given set of factors is the *signal space* defined by those factors. The *dimensionality* of the signal space is the number of factors required to span the space to account for a predetermined percentage of energy of the original set of signals. Principal component analysis is a method of factor analysis that offers certain computational and other advantages (*58*). This method accounts for the variance in the signal space so as to maximize the amount of variance derived from each successive factor. The solutions to principal component analysis are not unique, but arbitrary. Various rotations of this set of principal factors can be defined, just as the quadrants of the compass might be defined in various ways. We have found varimax rotation to yield factor orientations which correspond best to physiological processes (*59*). In order to compare AER's from different individuals under the same conditions or from the same individual under different conditions, procedures must be devised to ensure that the same factor waveforms are used to describe different bodies of data.

Figure 2 illustrates factor analysis of the six AER's in the top row. Three varimax factor waveforms are in the left column. The second row shows the contributions of the first factor to each of the original data waveshapes, obtained by multiplying the factor waveshape by the correlation coefficient between it and each data waveshape. The third row rep-

resents the first residuals obtained by subtracting the contribution of the first factor from each data waveshape. In subsequent rows this process is repeated for the second and third factors. The final residuals represent the energy in the original AER's unaccounted for by linear combination of the three factors.

As the number of AER's from different electrodes in cats increased, the number of factors necessary to span the signal space reached an asymptote (*52*). Similar data compression was achieved in analysis of AER's to flashes obtained from a monopolar occipital derivation in 70 normal human subjects. By means of a clustering procedure (*60*), five clusters of AER's were obtained and submitted to principal component analysis (*61*). Only two factors accounted for better than 85 percent of the energy. We then carried out varimax rotations on AER's obtained from ten derivations in each of ten normal subjects. For each subject, as few as two and no more than three factors were needed to account for an average of 94 percent of the energy (*62*).

Thus, under these conditions a limited variety of AER's exist in normal subjects. Interindividual variations, as well as intraindividual variations between various areas, could be described by a few factors. We realized that these inter- and intraindividual factors might be reconciled to describe AER's obtained from any derivation on any normal subject. When AER's from ten derivations on each of 48 normal subjects were factor analyzed, eight factors accounted for 98 percent of the energy of the total of 480 AER's (*63*). As a first approximation, this set of normal factors was capable of describing any AER to flash stimuli that was recorded from any derivation in any normal subject, and defined the signal space of normal subjects.

Stepwise factor analysis. This is a method in which factors from one set of data are used to describe another set. The method reveals very clearly the effects of dysfunction or treatment; for example, we have used this procedure to evaluate drug effects as follows:

1) The AER's are obtained under standard conditions prior to drug administration. The normal factors that account for this normal signal space are identified.

2) At a specified time after drug administration and under the same standard conditions, AER's are again obtained. These new waveshapes are regressed on the normal factors and the percentage of energy in the responses after drug administration that are within the normal signal space is computed. This procedure ensures comparability of the factor structure used to analyze the different data sets. On occasion, a drug causes shifts within the normal space, revealed as changes in the weightings of particular factors in AER's from certain anatomical regions. In other cases, a drug causes fundamental changes in morphology so that AER's from some regions can no longer be adequately described by the normal factors. A new "drug space" now exists, representing brain states caused by the drug, defined by the residual waveshapes after the contributions of the normal factors have been subtracted from the AER's after drug administration (Fig. 3).

Figure 4 illustrates the relative alteration in AER's from the visual cortex of a cat caused by different doses of several drugs, evaluated by stepwise factor analysis (*64*). The same method might be used to quantify the effects of a particular drug on different brain regions, or to provide a quantitative description of abnormal subspaces. Normative data bases can be constructed at various stages of development. Groups of patients with different brain dysfunctions provide a sample of abnormal data. The dysfunction space would be defined by the residuals outside the appropriate normal space. Numerical taxonomy of dysfunctions might be achieved by classifying

Table 3. Flow chart for stepwise factor analysis.

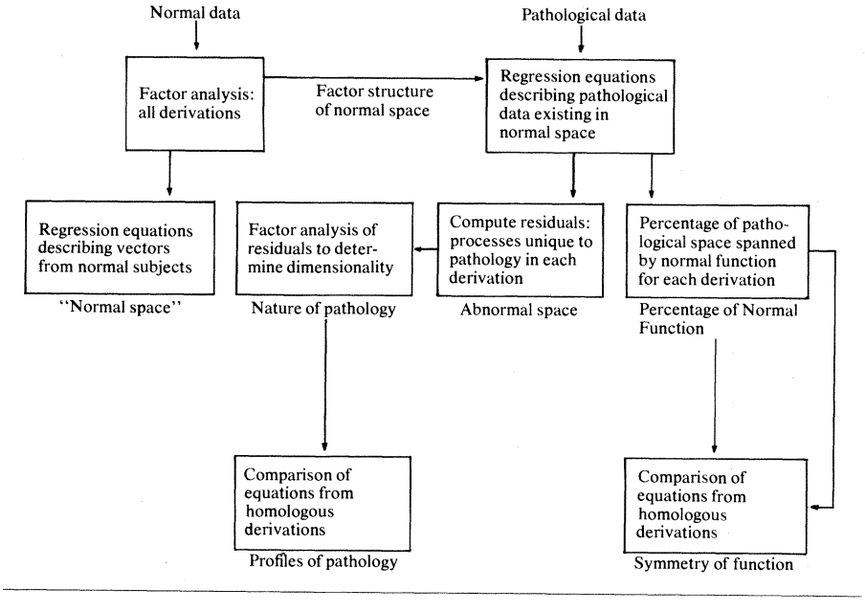

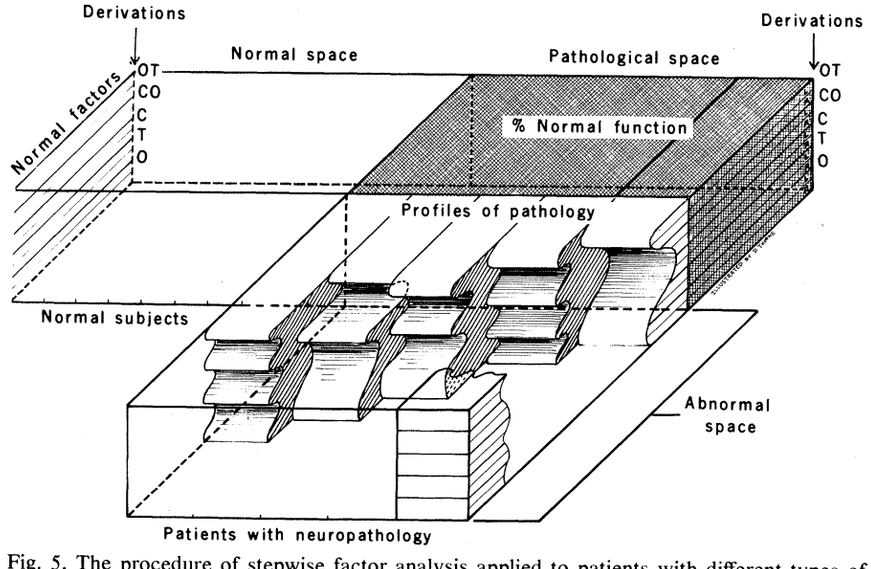

Fig. 5. The procedure of stepwise factor analysis applied to patients with different types of neuropathology.

the patterns of weightings of the dysfunction factors describing residuals from different dysfunctions. Such classification might not only aid diagnosis but might prove useful in prognosis or treatment evaluation by comparison of successive measures, and need not be restricted to brain dysfunctions (see Table 3 and Fig. 5).

Cluster analysis. *Z* transforms translate weighting coefficients describing AER morphology or other indices of the NB measure set into the relative probability of that index within the normal healthy population. A **Z** vector expressing the results of many measures can be constructed for any subject. There are many techniques for identifying clusters of data vectors in measure spaces.

We have used numerical taxonomic methods for the classification of single EP's and AER's from animals in behavioral situations, from neurological patients, normal and senile elderly patients, and normal and LD children. We were able to predict discriminative behavior in cats in a differential generalization paradigm by using multidimensional scaling (*65*) to classify single EP's (*56*). Multidimensional scaling was slightly superior to factor analysis, revealing greater clarity of structure. In other studies (*66*) we obtained clear clusters separating normal subjects from patients with tumors. Related methods currently under evaluation are projection pursuit (*67*), minimum spanning tree (*68*), and path analysis (*65*), which seems potentially useful to track an individual through the trajectory of development or remediation of a dysfunction.

Detection of Neurological Disease by Stepwise Factor Analysis

We have applied stepwise factor analysis to two groups of normal subjects and a variety of neurological patients (*69*), using a small subset of the NB, that is, routine EEG's and AER's to visual stimuli from bilateral central, occipital, temporal, centro-occipital, and occipito-temporal derivations (Table 4). We computed cross-correlation coefficient (*r*) between AER's from homologous derivations, the percentage of each AER (percentage regression) lying within the normal space defined by varimax factor analysis of the first group of normal subjects, and the asymmetry of weightings (regression asymmetry) in the regression equations for homologous AER's.

The results from the first normal group ($N = 50$) were used to define normal limits for each measure. By these criteria, one member of this normal group (2 percent) was erroneously categorized as "false positive." Next, the data from four test groups were analyzed: a new group of 25 normal subjects, 25 patients with confirmed brain tumors, 25 patients with cerebrovascular accidents (CVA), and 25 patients with epilepsy. The 75 neurological patients came from a much larger population and were selected to present a particularly stringent challenge; for example, ten tumor, ten CVA,

Table 4. Results of stepwise factor analysis (percentage regression and regression asymmetry), symmetry analysis and conventional EEG evaluation of normal subjects and three types of neurological patients. Criteria for abnormality: (i) Percentage regression: C ≤ 31, O ≤ 41, T ≤ 25, OT ≤ 20, CO not used (where C, O, T, OT, and CO are the central, occipital, temporal, occipito-temporal, and centro-occipital, respectively). (ii) Regression asymmetry (RA): total asymmetry of weightings for five homologous derivations > 310 percent. (iii) Symmetry analysis (*r*); $r_C \leq .59$, $r_O \leq .52$, $r_T \leq .26$, $r_{CO} \leq .81$, $r_{OT} \leq .16$. Symbols: −, negative; ?, doubtful; +, positive finding; †, false positive; ‡, false negative. For a positive diagnosis (ab), two different neurometric + values are required; if neurometric finding is only a single +, the conventional EEG must also be positive.

Test	Cases																								*N* detected by each index alone
	1	2	3	4	5	6	7	8	9	10	11	12	13	14	15	16	17	18	19	20	21	22	23	24	25	
Normal controls																										
% Regression	−	−	+	−	−	−	−	+	−	+	−	−	−	−	−	−	−	−	−	+	−	−	−	−	−	4
RA	−	−	−	−	−	−	−	−	−	−	−	−	−	−	−	−	−	−	−	−	−	−	−	−	−	0
r	−	−	−	−	−	−	−	−	+	−	−	−	−	−	−	−	−	−	−	−	−	−	−	−	−	1
EEG	−	−	−	−	−	−	−	−	−	−	−	−	−	−	−	−	−	−	−	−	−	−	−	−	−	0
Diagnosis from all measures	−	−	?	−	−	−	−	?	?	?	−	−	−	−	−	−	−	−	−	?	−	−	−	−	−	0 + 5 ? 0 †
Tumors																										
% Regression	−	+	+	+	−	+	−	+	−	+	−	+	−	−	+	+	+	+	−	+	+	+	−	+	+	16
RA	+	+	+	+	−	+	+	+	−	+	+	+	+	−	+	−	+	+	+	+	+	+	+	+	+	21
r	+	+	+	+	−	+	+	−	−	+	+	−	+	−	−	−	+	−	+	+	+	+	−	−	+	15
EEG	−	+	−	−	+	+	+	+	+	+	−	−	+	−	+	+	+	−	+	−	+	−	+	+	−	15
Diagnosis from all measures	ab	ab	ab	ab	?	ab	ab	ab	?	ab	ab	ab	ab	−	ab	ab	ab	ab	ab	ab	ab	ab	ab	ab	ab	22 + 2 ? 1 ‡
CVA																										
% Regression	+	+	+	+	−	+	−	+	+	+	−	−	−	−	−	−	+	+	+	−	−	−	−	+	−	12
RA	+	+	+	+	+	+	+	+	+	+	+	+	−	−	−	+	+	+	+	+	+	+	−	+	+	21
r	+	+	−	−	−	−	+	−	+	−	−	+	−	−	−	−	−	+	−	−	−	−	−	−	+	7
EEG	−	−	+	+	+	+	−	−	−	+	−	−	−	−	−	+	+	+	+	+	+	+	+	+	+	15
Diagnosis from all measures	ab	ab	ab	ab	ab	ab	ab	ab	ab	ab	?	ab	−	−	−	ab	ab	ab	ab	ab	ab	ab	?	ab	ab	20 + 2 ? 3 ‡
Epilepsy																										
% Regression	+	+	−	−	−	−	+	−	−	−	+	+	−	+	−	+	+	−	−	−	−	−	+	−	−	9
RA	−	−	+	+	−	+	−	+	−	+	+	−	+	−	+	−	+	−	−	+	+	+	+	+	−	14
r	−	−	+	+	−	+	−	−	−	−	−	−	−	−	+	−	−	−	−	−	−	−	−	−	−	4
EEG	−	+	+	+	−	+	+	+	+	−	+	+	+	+	+	+	+	−	−	+	+	+	+	+	+	20
Diagnosis from all measures	?	ab	ab	ab	−	ab	ab	ab	?	?	ab	ab	ab	ab	ab	ab	ab	−	−	ab	ab	ab	ab	ab	?	18 + 4 ? 3 ‡

and five epileptic cases appeared normal by conventional EEG criteria, and all of the epileptic patients were receiving effective anticonvulsant therapy.

For these four test groups, the same measures were computed, except that the AER's were regressed onto the normal factors according to the stepwise procedure. Each individual index was characterized as normal (−) or positive (+), according to the normal limits defined by the first normal group, as shown in the legend of Table 4. Any individual whose data included one positive finding was considered "at risk" or doubtful (?), while any two positive findings were sufficient for classification as abnormal (ab). Individuals with no positive findings were classified as normal (−). The classification of patients considered doubtful on the basis of neurometric assessment alone was resolved by taking the EEG into consideration. If the EEG findings were also positive, the patient was classed as abnormal.

A screening procedure. These results suggest that numerical taxonomy may already be a practical first step in a two-stage screening process. Patients classed as abnormal on the basis of a 2+ neurometric evaluation would be referred directly for neurological examination. Patients classified as doubtful would be referred for an EEG examination. Had this two-stage procedure been used in these 100 individuals, five healthy individuals would have been subjected to an unnecessary EEG examination, but no false positives would have resulted from the procedure as a whole. (By conventional methods, abnormal EEG findings would be expected in about 10 percent of a normal population.) Only 50 of the 75 neurological patients displayed abnormalities by conventional EEG criteria. Forty-two patients, 15 with normal conventional EEG's, were classified as abnormal on the basis of neurometric criteria alone; 21 more patients were classified as doubtful, of whom 18 were then classified as abnormal on the basis of positive findings in the conventional EEG. Thus, the two-stage method yielded 80 percent detection of the neurological disease cases with 0 percent false positives, while the conventional EEG alone only yielded 67 percent accuracy in these cases. Only five of the 12 cases considered normal by neurometric criteria displayed abnormalities in the EEG. Even if patients neurometrically classified as normal were not further examined, false negatives might be less than with exclusive reliance upon the conventional EEG. The two-stage method might thus lessen the number of EEG examinations required. These results might be substantially improved and extended to other difficult diagnostic problems by use of additional NB conditions and by AER techniques recently devised to detect specific brain diseases (*70*).

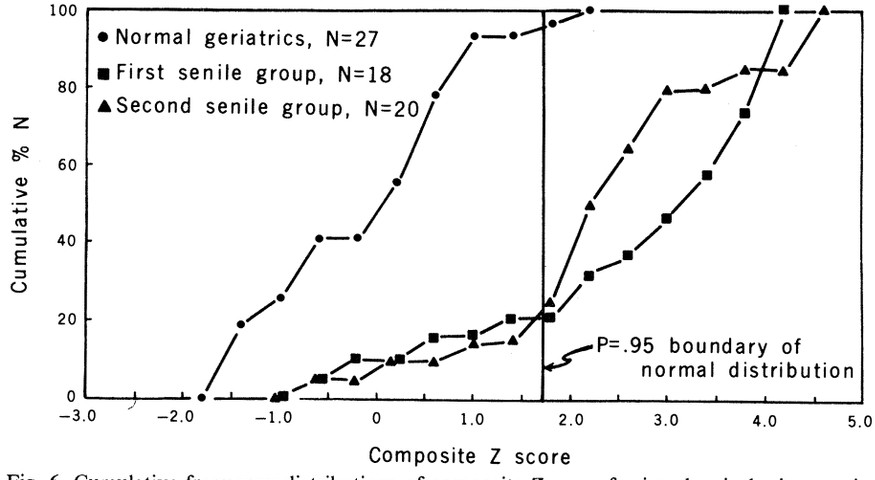

Fig. 6. Cumulative frequency distributions of composite **Z** score for interhemispheric covariance ($\overline{r^2}$) of AER to background flicker and clicks (conditions 7 and 9) and for log normal percentage power in the delta band of temporal and centro-temporal derivations (condition 1). Circles show data from first 27 normal elderly subjects; squares show data from first 18 senile subjects from initial study; triangles show data from 20 senile subjects from second study.

Neurometric Identification and Classification of Senile Individuals

We have used a modified subset of the NB to identify and classify 60 normal and 60 cognitively impaired patients (senile) over 60 years old (*2, 71*), using only subjects without overt neurological abnormalities or abnormal findings in a routine medical examination, including standard laboratory tests such as the SMA-12. All medication was suspended for at least 2 weeks before neurometric evaluation. Participants were considered "normal" if they had no history or current evidence of psychosis, long-term use of drugs acting on the brain, or pathology that might bias evaluations of brain function, and if they had a score of "not present" on seven scales of cognitive impairment in an "assessment of clinical status." These scales assessed confusion, mental alertness, recent memory, disorientation in time and place, mood depression, emotional lability, and capacity for self-care, and were accompanied by a psychiatric evaluation. The normal group was matched by sex, age, level of education, and ethnic background to the cognitively impaired group, comprised of persons with at least mild to moderate impairment on two or more assessment scales and with a "global impairment score" which exceeded a minimum value of 11.

In a collaborating laboratory (*72*), data were recorded on F-M magnetic tape under ten sequential conditions: (i) 2 minutes of spontaneous EEG; (ii) 5 minutes of click; (iii) 5 minutes of flash; (iv) 5 minutes of flash paired with click; (v) 1 minute of flash; (vi) 1 minute of click; (vii) 5 minutes of click while watching a silent color film; (viii) 2 minutes of click after the film; (ix) 5 minutes of flash while listening to a short story; and (x) 2 minutes of flash after the story. Subsequently, DEDAAS processed a playback of these data just like those from an online patient.

The EEG sample was submitted to spectral analysis, and AER's were computed from conditions (ii) through (x). From these data, 3696 neurometric indices were extracted for each subject. All measures were subjected to the appropriate Z transformation.

Separate discriminant functions were computed with the indices from each NB condition. Since so many measures were available, these discriminant functions predictably yielded highly accurate classifications whose concordance with clinical evaluations ranged from 64 to 86 percent. A multiple discriminant function, based on the two NB conditions which separately were most accurate, yielded an accuracy of 91 percent if subjects with ambiguous F ratios were excluded, and 96 percent if subjects with inconsistent psychiatric profiles were excluded. "Jackknife" replication of this function (*73*) yielded a replication accuracy of 84 percent ($P < .0001$).

Conventional EEG examination revealed abnormality in only 10 percent of the senile group, while discriminant function based only on neurometric EEG

indices showed 82 percent accuracy. Thus, neurometric methods seemed far more sensitive than the conventional EEG in identifying elderly people with cognitive impairments.

Our attention was drawn by the consistent differences between the two groups in AER symmetry, for late components between 200 and 500 msec. The mean cross-correlation ($\bar{r}$) was computed between homologous frontopolar-central, fronto-parietal, centro-temporal and centro-occipital derivations, and was markedly different for the two groups in that latency domain in every AER condition. Accordingly, a measure of interhemispheric asymmetry, mean covariance ($\bar{r}^2$), was computed for each subject in several AER conditions, and was plotted against the composite behavioral abnormality index obtained from the assessment of clinical status. Once a certain level of interhemispheric asymmetry was exceeded, the higher the asymmetry the greater was the behavioral abnormality. Preliminary studies suggest that *intra*hemispheric AER covariance may also be lower for the senile group.

The normal and senile groups showed no separation on comparable measures of EEG asymmetry. However, the two groups did differ significantly with respect to spectral analyses. The senile group showed a diffuse excess of activity in the delta band. Therefore, for a randomly selected subgroup of normal (N = 27) and senile (N = 18) individuals, the Z transforms of the interhemispheric covariance of late components of the AER elicited by background flicker and click (one per second) were combined with Z transforms of the log normal (ln) percentage of power in the delta band of the resting EEG from two derivations (temporal and central-temporal). The cumulative distributions of the two subgroups for this composite **Z** score were widely separated. A sample of moderately impaired elderly people (N = 20) was then recruited locally (*74*), neurometric data were gathered directly by DEDAAS, and the same composite measure was constructed. The results from the first study and this independent replication are shown in Fig. 6. Thus, normal and cognitively impaired elderly groups revealed marked neurometric differences not apparent in the conventional EEG, and showed a graded relation between abnormal neurometric indices and abnormal behavior, and these findings were replicated well in an independent sample as well as by the jackknife method.

Although these two groups as a whole were significantly different on most neurometric indices, different senile individuals were significantly abnormal on different indices. If distinctive profiles of abnormal neurometric indices were shared by subgroups of senile patients, these profiles might represent different organic causes of the same behavioral syndrome. Cognitive deficits due to these different causes might respond differentially to individualized types of treatment which might eventually be found. Accordingly, cluster analysis was used to fractionate the initial sample of 120 elderly people into different subgroups. Only NB data from conditions 1, 7, and 9 were used, as in the analysis described in Fig. 6. The innovative cluster analysis procedure is described elsewhere (*2*). The results are shown in Fig. 7. Seven clusters contained 101 people, while 19 remained unclassified. The first three clusters contained 45 normal and only two senile people, while the last four clusters contained 45 senile patients, seven patients who were probably senile but for whom full clinical assessment could not be obtained, and only two normals. The distribution within each cluster is shown in Table 5.

No significant differences were found between the four senile clusters with respect to severity of cognitive impairment. One of the normal groups displays an excess of slow waves in the EEG,

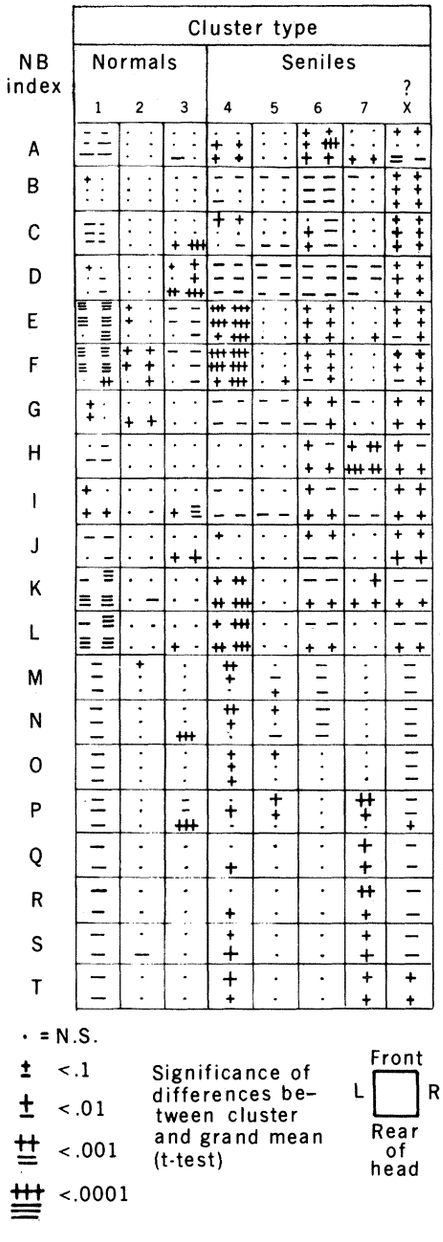

Fig. 7. Neurometric features distinguishing seven different clusters found within a sample of 120 elderly patients. Each column of rectangles shows the features displayed by members of the cluster indicated at the top of the column. Each row of rectangles indicates the values of a particular neurometric index extracted from a specific NB test condition, indicated at the left side of the row: *A*, signal strength, monopolar AER, condition 7; *B*, signal-to-noise ratio, monopolar AER, condition 7; *C*, signal strength, monopolar AER, condition 9; *D*, signal-to-noise ratio, monopolar AER, condition 9; *E*, percentage of delta power, monopolar EEG, condition 1; *F*, percentage of beta power, monopolar EEG, condition 1; *G*, signal-to-noise ratio, bipolar AER, condition 7; *H*, signal strength, bipolar AER, condition 7; *I*, signal-to-noise ratio, bipolar AER, condition 9; *J*, signal strength bipolar AER, condition 9; *K*, percentage of delta power, bipolar EEG, condition 1; *L*, percentage of beta power, bipolar EEG, condition 1; *M*, power asymmetry, monopolar AER, condition 7; *N*, power asymmetry, monopolar AER, condition 9; *O*, waveshape asymmetry, monopolar AER, condition 7; *P*, waveshape asymmetry, monopolar AER, condition 9; *Q*, power asymmetry, bipolar AER, condition 7; *R*, power asymmetry, bipolar AER, condition 9; *S*, waveshape asymmetry, bipolar AER, condition 7; *T*, waveshape asymmetry, bipolar AER, condition 9. Each rectangle represents a head viewed from the top, facing upward, analogous to Fig. 1B. Within each rectangle, the location of every entry corresponds to the anatomical location of the electrode or set of electrodes from which the measure was derived. Indices of symmetry are presented along the midline at a point corresponding to the anterior-posterior position of the regions which were compared. Every entry represents the value obtained by computing the Z transformation of each individual value, relative to the grand mean and standard deviation of the *total* sample, and then averaging across all the members of that cluster. The resulting average Z transform is presented as a symbol (see bottom of figure) whose sign shows the direction of deviation from the grand mean and whose size is proportional to the statistical significance of the deviation. The distribution of subjects by type within those different clusters is shown in Table 5. Nineteen subjects (13 normal, five senile, and one "unclassified") could not be located within any of these clusters by our methods, and are denoted as group ?/X.

usually considered characteristic of cerebral arteriosclerosis or diffuse cell loss, while at least one senile group fails to display these features. Thus, slow waves in the elderly may not reflect diminution of cerebral blood flow or diffuse loss of brain cells or, alternatively, such changes may be neither necessary nor sufficient for cognitive impairment. Three of the senile groups were noteworthy for interhemispheric AER asymmetry in long-latency components. Members of these clusters may suffer from impaired interhemispheric synchronization related to processing of information in the 200- to 500-msec latency domain. Individualized therapies may eventually be found for members of these groups.

Table 5. Members of normal (1 to 3) and senile (4 to 7) clusters found by cluster analysis [from (2)]

Category	Cluster							Subjects that did not cluster
	1	2	3	4	5	6	7	
Normal	30	9	6	2	0	0	0	13
Senile	1	1	0	15	13	10	7	5
No full clinical assessment	0	0	0	3	2	1	1	1
Total	31	10	6	20	15	11	8	19

Neurometric Identification and Classification of LD Children

The full NB described in Table 2 was initially administered to 118 children tentatively preclassified as "normal" and 57 preclassified as "learning disabled" based on school performance and opinions of the referral sources. The age of these male children ranged from 7.8 to 10.4 years. Testing was divided into several segments, interrupted at will for rest periods or meals. A total of 1 to 2 hours was required, depending on the restlessness of the child. An extensive psychometric battery was also administered (*75*), which usually occupied a full day. Test segments were intermingled with rest periods or lunch, or both. We will describe briefly here how these voluminous data were reduced and made comprehensible [details are provided elsewhere (*2, 53, 76, 77*)].

Data reduction. Means, standard deviations, and distributions were calculated for each measure for the whole sample. Variables displaying non-Gaussian distributions were submitted to a logarithmic transform. Every index extracted from each individual was then Z transformed relative to the sample means, to estimate its relative probability. Displays such as that in Fig. 1A enabled the distribution of values for any index at each electrode location to be compared for the normal and LD groups. Numerous significant univariate differences were thus found between the normal and LD groups. Displays such as that in Fig. 1B revealed the anatomical distribution of unusual indices in each child.

Comparison of neurometric and psychometric tests. Only the first two conditions of the NB (1 minute each of eyes open and of eyes closed EEG) were selected for this comparison because these measures can be obtained from almost every subject. We have obtained these measures successfully from over 1000 children from infancy to adolescence, with failure in less than ten cases. If effective discrimination between normal and LD groups could be accomplished with only these measures, this might be the basis for rapid and economical mass screening, applicable even to the extremely young or extremely impaired child.

Neurometric indices were extracted separately for the eyes open and eyes closed conditions and for the differences between the two conditions. Factor analysis was carried out on the full set of indices. Factor scores were computed for every factor for each individual and added to the measure set. Two discriminant functions were then computed with the use of this expanded set of neurometric EEG indices and with those psychometric measures which by univariate analysis of variance and stepwise discriminant methods discriminated best between the normal and LD groups (*53*).

The initial discriminant accuracy was 93 percent for the neurometric and 76 percent for the psychometric indices. The Jacknife replication accuracy was, respectively, 77 percent and 71 percent. When corrected for correlation with socioeconomic status (SES), culture, age, and WISC full-scale IQ, the neurometric discriminant score accounted for 4.6 times more independent variance than the psychometric score (23 versus 5 percent). Regression analysis of covariance revealed no significant covariance between the two kinds of discriminant scores, confirmed by absence of significant canonical correlations between the two measure sets.

Neurometric EEG measures not only discriminated between normal and LD children better and were more concordant with preclassification than the psychometric measures, but reflected processes more intimately related to brain function. Not only do psychometric measures in this study account for little of the independent variance related to the distinction between normal and LD children, but their relation to brain function is far more inferential. These findings cast doubts on whether these psychometric measures, which included many tests commonly used to assess for organicity in learning disability, possess any significant specific sensitivity to brain dysfunction. Aside from their bias with respect to age, IQ, culture, and SES, demonstrated above, the supposed relation between these psychometric measures and brain dysfunction may merely reflect the fact that performance on these tasks is heavily dependent upon skills which are difficult for the LD child to acquire.

The distribution of scores on the neurometric and psychometric discriminant functions was examined by plotting the value of one score versus the other for each child. The density of subjects at each point in this dual-discriminant space was represented as height on a probability surface. Computer-constructed views of this surface from eight different vantage points are presented in Fig. 8.

Multivariate procedures. We used factor analysis to reduce the highly redundant measure set described above to more manageable size, and stepwise discriminant analyses to identify the measures most sensitive to differences related to learning disabilities. For each NB item, least squares analysis of variance (ANOVA) across all derivations was used to identify independent latency bands along the analysis epoch in which AER's for the normal and LD subgroups were maximally different. More precise clustering could be achieved by restricting analyses to these sensitive latency bands, since less informative data were thus excluded. Independent corroborations of the ANOVA results were obtained as follows: The factor structure of the AER set for each condition was determined. Factor scores for every factor were computed for every derivation. Discriminant functions were then constructed with the use of weighted factor loadings at each latency point along the

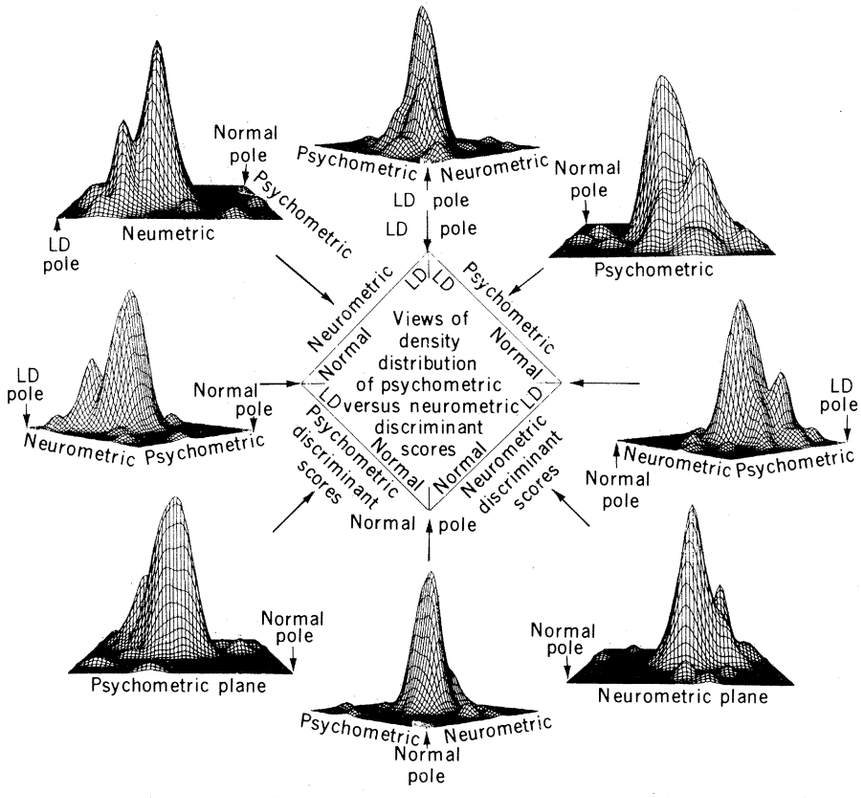

Fig. 8. Density distribution of psychometric versus neurometric discriminant scores. The two scores for each subject have been plotted with respect to a psychometric and neurometric axis. The surfaces illustrated represent the number or density of subjects whose scores fell at the corresponding points. These surfaces are presented as if viewed from different vantage points, to permit visualization of the distribution.

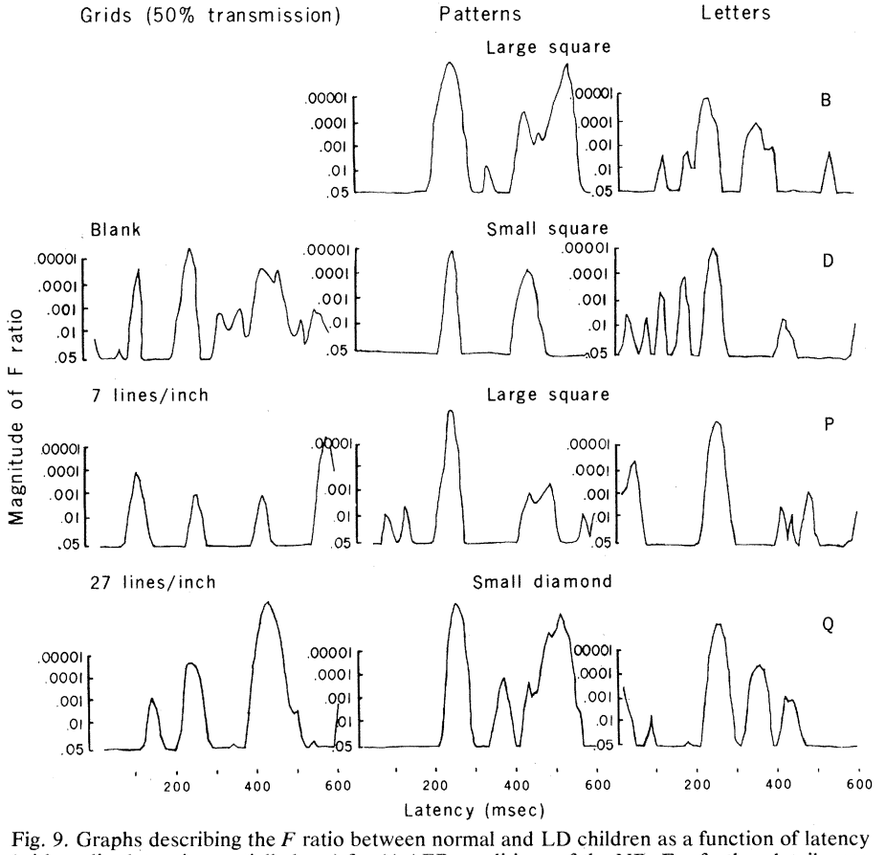

Fig. 9. Graphs describing the F ratio between normal and LD children as a function of latency (with earlier latencies partialled out) for 11 AER conditions of the NB. For further details, see text.

analysis epoch, describing the time course of differences between the normal and LD groups at every electrode placement for each NB item (*78*). These discriminant functions were compared with the F ratios obtained at each latency from the ANOVA, to confirm the latency bands in which the normal and LD groups could best be distinguished.

Differences between normal and LD children. In short, all of these multivariate analyses revealed highly significant differences between the normal and LD groups as a whole. Each graph in Fig. 9 shows the F ratio yielded by ANOVA for a different AER condition of the NB; all peaks are highly significant. The effects of early differences were partialled out of later values, so that all successive peaks were independent of prior peaks, at least at $P \leq .01$. Note that NB conditions in the same set gave peaks at similar latencies. Since entirely different data were used for each graph, these results constitute independent replications within each set. However, different sets of conditions gave peaks at different latencies, which may reflect the time at which critical steps in information processing take place in these different conditions.

Homogenous subgroups within the heterogeneous LD population. Figure 8 suggests that the population is more heterogeneous with respect to neurometric than psychometric measures. Projection of the surface onto the neurometric axis reveals clear multiple peaks. The heterogeneity of the LD group, suggested by this display, is borne out by cluster analysis. Data obtained from 50 LD children in three different EP conditions were subjected to cluster analysis by the same method used for our senile data, the entire AER waveshape being used as well as segments restricted to the latency bands found to be most discriminating by the ANOVA and discriminant technique above. Cluster analysis revealed five distinct subgroups within the group of LD children previously considered homogeneous. The AER's in the three different EP conditions displayed distinctive features for each subgroup.

The sample of LD children in this study was far too small and the age range too restricted for accurate estimation of the actual number of subgroups within the LD population. Further, much more extensive behavioral and neuropsychological assessment was desirable to identify the functional significance of membership in any cluster. Accordingly, a study was initiated in a school for educationally handicapped children (*79*). The full NB has already been adminis-

tered to over 750 children, and more extensive behavioral evaluations are in progress.

In view of the discriminating power of the neurometric EEG indices revealed in our initial study of LD children, and in view of the sensitivity of measures of hemispheric asymmetry revealed in our studies of cognitive impairment in the elderly, we carried out a preliminary analysis of comparable NB data from the first 533 of these children. For this analysis, we used the EEG frequency and symmetry measures and EP symmetry measures which contributed most to the previous discriminant functions in an attempt to replicate our earlier findings.

Briefly, a polynomial regression was computed to fit the set of values for power in the various EEG bands as a function of age and electrode derivation published by Matoušek and Petersén (*6*). For each frequency band and electrode derivation, this procedure yielded a smoothed regression function based on 561 subjects. We think these smoothed spectral estimates are more reliable than the original data from which they are derived. The original data were based on sample sizes ranging from 18 to 41 subjects at each age. The regression function offers the further advantage of allowing interpolation of values corresponding to the actual age of any child, while the original data were quantized into yearly increments. These polynomial functions agreed well with comparable data obtained from 85 children considered as unequivocally normal in our initial study. Minor adjustments were made to compensate for possible differences in our equipment, measurement procedures, and for the greater ethnic heterogeneity of our sample population. Means and standard deviations for EEG and AER symmetry were taken from our previous study, which agreed well with other findings (*7, 15*).

Using these normative data, we subjected to Z transformations the EEG indices and AER indices (obtained in response to blank flashes and spatial grids with 27 and 7 lines per inch) from 533 LD and 50 normal children randomly selected from our initial normal sample. Indices with Z-transform values ≥ 1.96 ($P \leq .05$) were defined as "dysfunctional" and tallied separately for bilateral parieto-occipital (PO), central (C), and temporal (T) derivations. The AER indices were only considered dysfunctional if the same index was deviant in the same latency domain in the same region for at least two out of three of the AER conditions.

The 533 LD children were randomly divided into two groups, LD_1 (265 cases) and LD_2 (268 cases). The members of each group were then classified separately according to the seven regional categories (columns) and seven dysfunction categories (rows) shown in Table 6. A coefficient of concordance was computed between these two independent distributions and was found to be 0.991 ($P < 10^{-6}$). The data from LD_1 and LD_2 were then combined, and converted to percentages. Table 6 reveals marked differences between the normal LD subgroups: 92.6 percent of the LD group but only 20 percent of the normal group showed unusual indices significant at the $P < .05$ level. Unusual values in the normal group were always restricted to only one anatomical region (PO or T) and consisted of dysfunction in a single index. Only 5.5 percent of the LD group showed this pattern of dysfunction; 77.3 percent of the LD group but 0 percent of the normal group showed dysfunctions in more than one anatomical derivation, with 50.8 percent of the LD children displaying dysfunctions in every anatomical region.

Nine major clusters contained over 64.3 percent of the LD children but 0 percent of normal children. Five patterns of dysfunction (rows) accounted for 82 percent of the LD children but 0 percent of normals, while 81.1 percent of the LD's and 0 percent of the normal children displayed dysfunction in five anatomical patterns (columns). Unusual EEG features were shown by 78.3 percent of the LD children but only 20 percent of the normal children, thus replicating our original finding that normal and LD children differ markedly with respect to certain neurometric EEG indices. Note that 87.5 percent of the LD children but only 8 percent of the normal children displayed abnormal EEG or AER asymmetry, or both, with 71 percent of LD's but 0 percent of normals showing AER asymmetry, consistent with our finding of marked AER asymmetry in many cognitively impaired elderly persons. A much larger sample of normal children must now be studied to obtain normative data over a wider age

Table 6. Frequency distribution of 533 LD and 50 normal (N) children according to anatomical location (columns) and types of neurometric dysfunction (rows) significant at the $P \leq .05$ level (PO, parieto-occipital; C, central; and T, temporal derivations).

Anatomical location of dysfunction														Total	
PO		C		T		PO + C		PO + T		C + T		PO + C + T			
N	LD	N	LD	N	LD	N	LD	N	LD	N	LD	N	LD	N	LD
EEG frequency															
.060	.004	.000	.011	.060	.006	.000	.004	.000	.002	.000	.009	.000	.015	.120	.051
EEG asymmetry															
.040	.006	.000	.000	.040	.039	.000	.000	.000	.004	.000	.000	.000	.004	.080	.053
EEG frequency and EEG asymmetry															
.000	.000	.000	.004	.000	.006	.000	.000	.000	.045*	.000	.009	.000	.047*	.000	111*
EP asymmetry															
.000	.030*	.000	.017	.000	.015	.000	.034*	.000	.008	.000	.009	.000	.030*	.000	.143*
EEG frequency and EP asymmetry															
.000	.000	.000	.004	.000	.000	.000	.009	.000	.008	.000	.006	.000	.073*	.000	.099*
EEG asymmetry and EP asymmetry															
.000	.000	.000	.002	.000	.004	.000	.011	.000	.017	.000	.017	.000	.071*	.000	.122*
EEG frequency and EEG asymmetry and EP asymmetry															
.000	.000	.000	.000	.000	.006	.000	.009	.000	.045*	.000	.019	.000	.268*	.000	.347*
Total															
.100	.039	.000	.038*	.100	.075	.000	.068*	.000	.128*	.000	.069*	.000	.508*	0.200	0.926
No dysfunction														0.800	0.058

* Significantly more LD than normal. †Nine LD cases had inadequate data (.016).

range, since most of our normals were 9 years old, and to confirm the low incidence of false positives with the criteria used in this study (*80*).

The most striking feature of these results is the high percentage of LD children who displayed multiple types of dysfunction in multiple regions. The high incidence of pervasive dysfunction suggests widespread occurrence of some source of severe, generalized insult, such as pre- or perinatal trauma, malnutrition, or stimulus deprivation. Careful retrospective and longitudinal studies might give some insight into the cause of such dysfunction, and preventive measures might then be devised. Certain abnormal patterns were found predominantly in children less than 12 years old, while others were found mostly in teen-agers. These patterns may merely be a sampling error, reflecting changing criteria in school evaluation policies, or may be related to the concept of developmental lag (which may explain why the common prediction of the pediatrician, "this child will grow out of it," is so often correct) or to obscure endocrine influences at the onset of puberty.

Differential neurometric profiles of specific learning disabilities. Using the concept of the "learning quotient" first put forward by Myklebust (*81*), which evaluates the academic achievement of a child relative to his mental age, chronological age, and grade level separately for different skills, Ahn (*82*) conducted an analysis of 20 normal children, ten children with defective language but normal arithmetic skills (verbal underachievers, or VUA), ten children with defective arithmetic but normal language skills (arithmetic underachievers, or AUA), and ten children with both defective language and arithmetic skills (mixed underachievers, or MUA), selected from the subgroup of children 9 years old in our initial study. By means of ANOVA, the AER's of the normal children were compared to those from the combined group of underachievers (LD), the VUA, AUA, and MUA groups, separately for all left-hemisphere and right-hemisphere placements for each of the 11 NB conditions for which the overall normal versus LD differences were illustrated in Fig. 9.

Figure 10 shows the results of these ANOVA comparisons between normal children and children with different types of learning disabilities. Although F ratio differences significant at the $P \leq .01$ level are evident when the combined LD group is compared to the normals, no clear hemispheric pattern emerges. This provides an example of how treatment of a heterogeneous population as homogeneous can obscure rather than clarify diagnostic features. The data for normal versus VUA show that differences between these two groups are primarily found on the left hemisphere, mostly between 300 and 450 msec. The data for normal versus AUA show a pattern which is very different and remarkably consistent, with significant F ratios in the 300- to 350-msec latency domain on the right hemisphere for all 11 conditions. The data for normal versus MUA show significant F ratios almost exclusively restricted to the 225- to 250-msec domain on the left hemisphere for all 11 conditions.

Thus, the three different types of underachievers display three radically and replicably different patterns of deviation from the AER morphology observed in children with normal learning quotients. The neurometric features of two of the five subgroups classified by the cluster analysis of the LD sample described earlier were closely similar to the features of the AUA and MUA subgroups just discussed. A remarkable feature of these findings is that information processing in children with a particular type of learning disability seems to reflect a general operational defect, independent of the specific information content of the input, revealed as a distinctive spatiotemporal pattern.

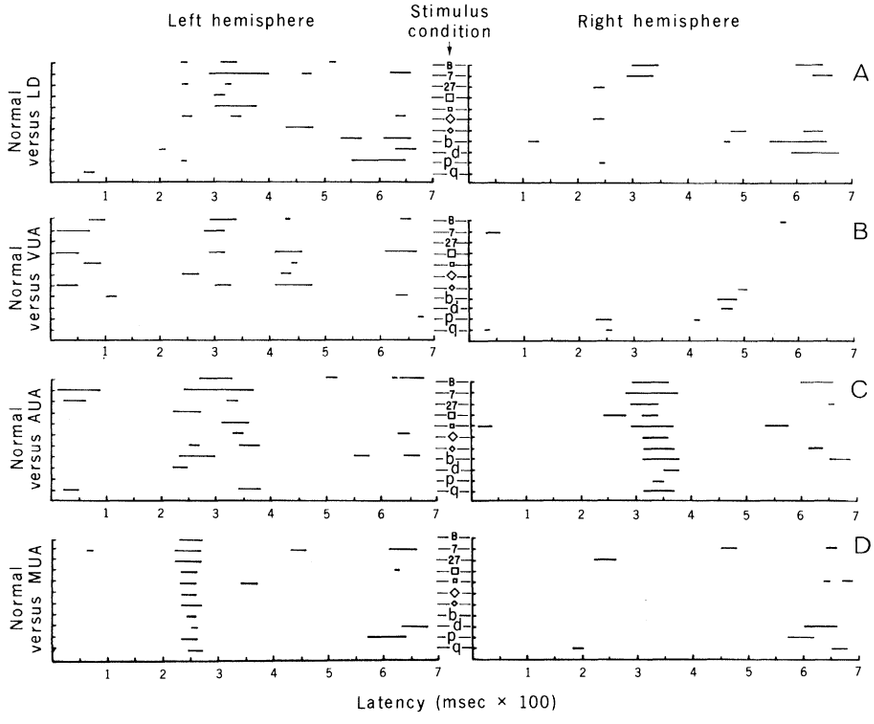

Fig. 10. Results of ANOVA comparisons, as shown in Fig. 9, between (A) 20 normal children and a group of LD children containing ten verbal underachievers (VUA), ten arithmetic underachievers (AUA), and ten underachievers in both verbal and arithmetic skills (MUA); (B) the 20 normal and ten VUA children; (C) the 20 normal and ten AUA; and (D) the 20 normal and ten MUA. The graphs on the left side show differences for all combined left-hemisphere electrode placements, while those on the right show right-hemisphere differences. In each graph, the horizontal bars indicate the latency regions in which the F ratios between the compared samples were significant at $P < .01$. Each graph presents the results of separate ANOVA evaluations for 11 different NB conditions, identified by vertical sequence down the center of the figure. Clear spatiotemporal differences in AER's exist between the normals and each of the groups of differently disabled children, and each specific type of disability is characterized by a distinctive spatiotemporal pattern (*82*).

Conclusions

Neurometric methods may serve to provide criteria for the efficacy of interventions, whether pharmacological or behavioral, in a wide variety of diseases and dysfunctions, including neurological disease, senile deterioration, learning disability, psychosis, mental retardation, drug addiction, and malnutrition. The amount of damage and rate of recovery from perinatal trauma, head injury, and stroke may be quantitatively evaluated and followed by neurometrics. These techniques may also be used to assess the consequences of organic diseases not directly but potentially relevant to brain function, such as cardiovascular disease, kidney disease, and various metabolic diseases and to determine the effects on human beings of drugs, food additives, toxins, and environmental pollution.

Once banks of data are constructed from different types of normal and abnormal individuals, and effective mass screening programs are inaugurated, neurometrics may prove useful for many of these purposes. The early detection and remediation of brain disease and cognitive disorders would reduce some of the human social and economic costs of failure to recognize these problems. A real peril exists, however, in that the fate of young as well as old persons might be as decisively influenced by neurometric measures as has been the case with psychometric measures. While it may eventually be possible to achieve early identification of children at risk for specific learning disabilities before behavioral difficulties have emerged, the attendant dangers of premature or mistaken diagnosis and the adverse effects of labeling a child as dysfunctional must be clearly recognized. Procedures must be devised to ensure that neurometric evaluations are used to optimize the development of individuals, rather than to restrict their opportunities as has too often been the case with psychometric assessment.

References and Notes

1. E. Donchin and D. B. Lindsley, *Average Evoked Potentials* (National Aeronautics and Space Administration, Publ. NASA SP-191, Washington, D.C., 1969); D. Regan, *Evoked Potentials in Psychology, Sensory Physiology and Clinical Medicine* (Wiley-Interscience, New York, 1972).
2. E. R. John, *Functional Neuroscience*, vol. 2, *Neurometrics*, E. R. John and R. W. Thatcher, Eds. (Lawrence Erlbaum Associates, Hillsdale, N.J., in press).
3. F. F. De la Cruz, B. H. Fox, R. H. Roberts, Eds., "Minimal brain dysfunction," in *Ann. N.Y. Acad. Sci.*, (1973), vol. 205; P. H. Wender, *Minimal Brain Dysfunction in Children* (Wiley-Interscience, New York, 1971).
4. R. Conely, *The Economics of Mental Retardation* (Thomas, Springfield, Ill., 1973); HEW National Advisory Committee on Dyslexia and Related Reading Disorders, *Reading Disorders in the United States* (Department of Health, Education, and Welfare, Washington, D.C., 1969); B. L. Kratoville, *Youth in Trouble* (Academic Therapy Publications, San Rafael, Calif., 1974); M. Menkes, J. S. Rowe, J. H. Menkes, *Pediatrics* **39**, 393 (1967); U.S. Bureau of the Census, *Statistical Abstract of the United States, 1971 Census* (Washington, D.C., ed. 92, 1971).
5. B. Braginsky and M. Braginsky, *Mainstream Psychology: A Critique* (Holt, Rinehart & Winston, New York, 1973); E. Zigler and L. Phillips, *J. Abnorm. Soc. Psychol.* **63**, 66 (1961).
6. M. Matoušek and I. Petersén, *Automation of Clinical Electroencephalography*, P. Kellaway and I. Petersén, Eds. (Raven, New York, 1973).
7. T. Harmony, T. Otero, J. Ricardo, G. Fernandez, *Brain Res.* **61**, 133 (1973).
8. A. J. Capute, E. F. L. Niedermeyer, F. Richardson, *Pediatrics* **41**, 1104 (1968); R. Cohn and J. Nardini, *Am. J. Psychiatry* **115**, 44 (1958); C. K. Conner, *Psychophysiology* **7**, 418 (1971); J. R. Hughes, in *Progress in Learning Disabilities*, H. R. Myklebust, Ed. (Grune & Stratton, New York, 1968), vol. 1, p. 113; J. Hughes and H. Myklebust, unpublished results; J. Hughes and G. Park, unpublished results; G. Otero, T. Harmony, J. Ricardo, *Act. Nerv. Super.* **17**, 120 (1975); R. Pavy and J. Metcalfe, *Electroencephalogr. Clin. Neurophysiol.* **19**, 414 (1965); L. Sorel, P. Lebrun, G. Leotard, F. Delaite, M. Rucquoy-Ponsar, G. Basecqz, D. de Biolley, *ibid.* **18**, 633 (1965); A. Wikler, J. F. Dixon, J. B. Parker, Jr., *Am. J. Psychiatry* **127**, 634 (1970).
9. G. Otero, J. Harmony, J. Ricardo, *Act. Nerv. Super.* **17**, 127 (1975).
10. T. Harmony, G. Otero, J. Ricardo, P. Valdes, G. Fernandez, in *Symposium on Applications of Computation in the Study of the Nervous System* (National Scientific Research Center of Cuba, Havana, 1975); P. Kellaway and I. Petersén, Eds., *Automation of Clinical Electroencephalography* (Raven, New York, 1973); D. O. Walter and M. A. B. Brazier, Eds., "Advances in EEG Analysis," in *Electroencephalogr. Clin. Neurophysiol. Suppl. 27* (1969).
11. M. Matoušek and I. Petersén, *Electroencephalogr. Clin. Neurophysiol.* **35**, 603 (1973).
12. J. Ricardo, P. Valdes, T. Harmony, *Symposium on Applications of Computation in the Study of the Nervous System* (National Scientific Research Center of Cuba, Havana, October, 1975).
13. B. K. Bagchi and K. A. Kooi, *Electroencephalogr. Clin. Neurophysiol.* **13**, 180 (1961); J. Bancaud, J. Talairach, A. Bonis, M. Bordas Ferrer, *ibid.* **29**, 100 (1970); R. I. Birchfield, W. P. Wilson, A. Heyman, *Neurology* **9**, 859 (1959); W. A. Cobb, in *Electroencephalography, The EEG of Specific Lesions*, E. Hill and G. Parr, Eds. (Macdonald, London, 1963), p. 295; F. A. Gibbs and E. L. Gibbs, *Atlas of Electroencephalography* (Addison-Wesley, Cambridge, Mass., 1964), vol. 3, p. 337; T. Mircea, A. Naghin, E. Gergely, P. Corbin, *Electroencephalogr. Clin. Neurophysiol.* **31**, 525 (1971); M. Velasco, M. López, G. Zenteno Alanis, F. Velasco, *Arch. Invest. Med.* **1**, 93 (1970).
14. G. Otero, T. Harmony, J. Ricardo, in preparation.
15. T. Harmony, J. Ricardo, G. Otero, G. Fernandez, S. Llorente, P. Valdes, *Electroencephalogr. Clin. Neurophysiol.* **35**, 232 (1973).
16. L. E. Rhodes, R. E. Dustman, E. C. Beck, *ibid.* **26**, 232 (1969).
17. L. Bergamini, B. Bergamasco, L. Fra, G. Gandiglio, R. Mutani, *ibid.* **22**, 260 (1967); E. Callaway, *J. Nerv. Ment. Dis.* **143**, 80 (1966); E. J. Jonkman, thesis, University of Amsterdam (1967); H. G. Vaughan, R. Katzman, J. Taylor, *Electroencephalogr. Clin. Neurophysiol.* **15**, 737 (1963).
18. T. Harmony, postdoctoral thesis, Centro Nacional de Investigaciones Cientificas de la Universidad de la Habana, La Habana, Cuba (1977).
19. R. M. Copenhaver and N. M. Perry, Jr., *Invest. Ophthalmol.* **3**, 665 (1964); H. Davis, S. K. Hirsch, J. Shelnutt, C. Bowers, *J. Speech Hear. Res.* **10**, 717 (1967); R. G. Eason, C. T. White, N. Bartlett, *Psychonom. Sci.* **2**, 113 (1970); M. R. Harter, *Vision Res.* **10**, 1365 (1971); ——— and C. T. White, *Electroencephalogr. Clin. Neurophysiol.* **28**, 48 (1969); W. D. Keidel and M. Spreng, *J. Fr. Oto Rhino Laryngol.* **19**, No. 1 (1970); I. Rapin and L. J. Graziani, *Neurology* **17**, 881 (1967).
20. E. R. John, *Ann. Ophthalmol.* **6**, 55 (1974).
21. R. Spehlmann, *Electroencephalogr. Clin. Neurophysiol.* **19**, 560 (1965); M. R. Harter, *Vision Res.* **8**, 701 (1968); D. A. Jeffreys, *Neurosci. Res. Program Bull.* **7**, (1969); D. M. Mackay and D. A. Jeffreys, *Handbook of Sensory Physiology* (Springer-Verlag, Berlin, 1971); W. J. Rietveld, W. E. M. Tordoir, J. R. B. Hagenouw, J. A. Lubbers, Th. A. C. Spoor, *Acta Physiol. Pharmacol. Neerl.* **14**, 259 (1967); L. H. Van Der Tweel, D. Regan, H. Speckreijse, *ISCERG Symposium*, Istanbul (1970).
22. E. Callaway, in *Behavior and Brain Electrical Activity*, N. R. Burch and H. L. Altshuler, Eds. (Plenum, New York, 1974); G. Lelord, *Proceedings of Colloque Inserm on Average Evoked Responses and Their Conditioning in Normal Subjects and Psychiatric Patients* (Inserm, Tours, France, 1972); C. Shagass, in *ibid.*
23. R. Kirk, *Br. J. Psychiatry* **114**, 1509 (1968).
24. D. A. Burkhardt and L. A. Riggs, *Vision Res.* **7**, 453 (1967); L. A. Riggs and C. E. Sternheim, *J. Opt. Soc. Am.* **59**, 635 (1969); T. Shipley, R. W. Jones, A. Fry, *Science* **150**, 1162 (1965).
25. M. Clynes, M. Kohn, J. Gradijan, *IEEE Int. Conv. Dig.* (1967); E. R. John, R. N. Herrington, S. Sutton, *Science* **155**, 1439 (1967).
26. C. Fields, *Science* **165**, 1377 (19➡ K. H. Pribram, D. N. Spinelli, M. C. Kamback, *ibid.* **157**, 94 (1967).
27. Y Akiyama, F. J. Schulte, M. A. Schultz, A. H. Parmelee, *Electroencephalogr. Clin. Neurophysiol.* **26**, 371 (1969); O. D. Creutzfeldt and U. Kuhnt, *ibid. Suppl. 29* (1967); R. E. Dustman and E. C. Beck, *ibid.* **26**, 2 (1969); R. J. Ellingson, *ibid.* **21**, 403 (1966); T. P. Fogarty and R. N. Reuben, *Arch. Ophthalmol.* **81**, 454 (1969); A. Hrbek, M. Hrbkova, H. G. Lenard, *Electroencephalogr. Clin. Neurophysiol.* **26**, 597 (1969); H. G. Lenard, H. von Bernuth, S. J. Hutt, *ibid.* **27**, 121 (1969); H. Umezaki and F. Morell, *ibid.* **28**, 55 (1970).
28. D. Giannitrapani, *Electroencephalogr. Clin. Neurophysiol.* **27**, 480 (1969); L. E. Rhodes, R. E. Dustman, E. C. Beck, *ibid.* **26**, 237 (1969).
29. M. Buschbaum and P. Fedio, *ibid.*, **26**, 266 (1969); *Physiol. Behav.* **5**, 207 (1970); S. A. Shelburne, Jr., *Electroencephalogr. Clin. Neurophysiol.* **32**, 17 (1972).
30. R. Hernandez-Peon, H. Scherrer, M. Jouvet, *Science* **123**, 331 (1956).
31. V. L. Schwent and S. A. Hillyard, *Electroencephalogr. Clin. Neurophysiol.* **38**, 131 (1975).
32. F. Morrell and L. Morrell, in *The Analysis of Central Nervous System and Cardiovascular Data Using Computer Methods*, L. D. Proctor and W. R. Adey, Eds. (National Aeronautics and Space Administration, Washington, D.C., 1965).
33. H. Birch, in *Conference on Minimal Brain Dysfunction* (New York Academy of Sciences, New York, 1972), p. 77; T. Shipley and R. W. Jones, *J. Commun. Disord.* **2**, 295 (1969).
34. A. B. Barnet and A. Lodge, *Nature (London)* **214**, 252 (1967).
35. J. Grynberg and E. R. John, in *Consciousness and Self Regulation: Advances in Research*, I. G. Schwartz and D. Shapiro, Eds. (Plenum, New York, 1976), p. 21.
36. T. Teyler, A. Megela, G. Hess, in *Fourth International Congress on Event Related Slow Potentials of the Brain* (Plenum, New York, in press).
37. S. Sutton, M. Braren, J. Zubin, E. R. John, *Science* **150**, 1188 (1965).
38. R. W. Thatcher, in *The Neurobiology of Aging*, R. Terry and S. Gershon, Eds. (Raven, New York, 1976), pp. 43–102; P. Tueting, in *Fourth International Congress on Event Related Slow Potentials of the Brain* (Plenum, New York, in press); R. W. Thatcher and E. R. John, in *Behavior and Brain Electrical Activity*, N. R. Burch and H. L. Altshuler, Eds. (Plenum, New York, 1975), pp. 303–324.
39. S. Sutton, P. Tueting, J. Zubin, E. R. John, *Science* **155**, 1436 (1967).
40. J. S. Barlow, L. Morrell, F. Morrell, in *Proceedings of an International Colloquium* (Czechoslovakia Academy of Sciences, Prague, 1967); E. R. John, in *Information Storage and Neural Control*, W. S. Fields and W. Abbot, Eds. (Thomas, Springfield, Ill., 1963), p. 243; in *The Neurosciences: A Study Program*, G. C. Quarton, T. Melnechuk, F. O. Schmitt, Eds. (Rockefeller Univ. Press, New York, 1967), p. 690; R. Klinke, H. Fruhstorfer, P. Finkenzeller, *Electroencephalogr. Clin. Neurophysiol.* **26**, 216 (1969); D. S. Ruchkin and S. Sutton, *Bull. Psychonom. Soc.* **2**, 144 (1973); D. S. Ruchkin, S. Sutton, P. Tueting, *Psychophysiology* **12**, 591 (1975); H. Weinberg, W. Grey-Walter, H. H. Crow, *Electroencephalogr. Clin. Neurophysiol.* **29**, 1 (1970).
41. E. R. John, *Science* **177**, 850 (1972).
42. ———, F. Bartlett, M. Shimokochi, D. Kleinman, *J. Neurophysiol.* **36**, 893 (1973).
43. W. Brown, J. Marsh, J. Smith, *Behav. Biol.* **9**, 755 (1973); W. S. Brown, J. T. Marsh, J. C. Smith, *Electroencephalogr. Clin. Neurophysiol.* **41**, 113 (1976); T. Teyler, T. Harrison, R. Roemer, R. Thompson, *Psychonom. Soc. Bull.* **1**, 333 (1973).
44. V. L. Johnston and G. L. Chesney, *Science* **186**, 944 (1974).
45. H. Begleiter and A. Platz, *Psychophysiology* **6**, 91 (1969); E. R. John, *Mechanisms of Memory* (Academic Press, New York, 1967); ——— and R. W. Thatcher, Eds. *Functional Neuroscience* (Lawrence Erlbaum Associates, Hillsdale, N.J., in press); F. K. Killam and A. J. Hance, *Abstracts of the Proceedings of the 23rd International Congress of Physiological Science* (Tokyo, 1956), p. 1125; G. T. Sakhuilina and G. K. Merzhanova, *Electroencephalogr. Clin. Neurophysiol.* **20**, 50 (1966).
46. H. Fitzgerald and Y. Brackbill, *Psychol. Bull.* **83**, 353 (1976); M. Hofmann, B. Z. Karmel, M. Lester, *Proc. Soc. Neurosci.* (Society for Neuroscience, New York, 1975); H. Kaye in *Advances in Child Development and Behavior* (Academic Press, New York, 1967), vol. 3, p. 31; H. Papousek in *Behavior in Infancy and Early Childhood*, Y. Brackbill and G. G. Thompson, Eds. (Free Press, New York, 1967), p. 259; E. Siqueland and L. P. Lipsitt, in *Experimental Child Psychology*, H. Reese and L. P. Lipsitt, Eds. (Academic Press, New York, 1970), p. 65.
47. M. S. Preston, J. T. Guthrie, B. Childs, *Psychophysiology* **11**, 452 (1974).
48. L. S. Prichep, S. Sutton, G. Hakerem, *ibid.*, in press; J. H. Satterfield, *Sem. Psychiatry* **5**, 35 (1973).
49. M. Buchsbaum and P. Wender, *Arch. Gen. Psychiatry* **29**, 764 (1973); D. T. Shields, *J. Learn. Disabil.* **6**, 501 (1973).
50. H. B. Bigum, R. E. Dustman, E. C. Beck, *Electroencephalogr. Clin. Neurophysiol.* **28**, 576 (1970); G. Lelord, F. Laffont, P. Jusseaume, J. L. Stephant, *Psychophysiology* **10**, 415 (1973).
➡ C. K. Conners, *Child Dev.* **41**, 667 (1970); B. Saletu, M. Saletu, J. Simeon, G. Viamontes, T. M. Itil, *Biol. Psychiatry* **10**, 253 (1975).
52. E. R. John, D. S. Ruchkin, J. Villegas, *Ann. N.Y. Acad. Sci.* **112**, 363 (1964); E. Donchin,

IEEE Trans. Biomed. Eng. **BME-13**, 131 (1966).
53. E. R. John, B. Z. Karmel, L. S. Prichep, H. Ahn, M. John, in *Psychopathology and Brain Dysfunction*, C. Shagass, S. Gershon, A. Friedhoff, Eds. (Raven, New York, 1977).
54. J. E. Strauss, J. J. Bartko, W. T. Carpenter, *Br. J. Psychiatry* **122**, 531 (1973).
55. C. K. Conners, *Ann. N.Y. Acad. Sci.* **205**, 283 (1973).
56. E. L. Schwartz, A. Ramos, E. R. John, *Behav. Biol.* **17**, 109 (1976).
57. R. Asarnow, D. F. MacCrimmon, J. M. Cleghorn, R. A. Steffy, in *Second International Rochester Conference on Schizophrenia*, L. Wynne and R. Cromwell, Eds. (Wiley, New York, in press).
58. H. Harmon, *Modern Factor Analysis* (Univ. of Chicago Press, Chicago, 1960).
59. H. F. Kaiser, *Psychometrika* **23**, 187 (1958); E. R. John, P. Walker, D. Cawood, M. Rush, J. Gehrmann, *Int. Rev. Neurobiol.* **15**, 273 (1972).
60. D. Arnal, P. Gerin, D. Salmon, J-P. Nakache, P. Magnard, F. Peronnet, R. Hugonnier, *Electroencephalogr. Clin. Neurophysiol.* **31**, 365 (1971); D. Wishart, *Biometrics* **22**, 165 (1969).
61. P. Valdes, J. Ricardo, T. Harmony, in *Symposium on Applications of Computation to the Study of the Nervous System* (National Scientific Research Center of Cuba, Havana, 1975).
62. T. Harmony, P. Valdes, E. R. John, in collaborative work carried out at National Scientific Research Center, Havana, Cuba, 1974.
63. T. Harmony, P. Valdes, E. R. John, P. Easton, H. Ahn, unpublished data, cited in (*2*).
64. E. R. John and S. Auerbach, unpublished results.
65. R. O. Duda and P. E. Hart, *Pattern Classification and Scene Analysis* (Wiley, New York, 1973); J. W. Sammon, Jr., *IEEE Trans. Comput.* **C-18**, 401 (1969).
66. E. R. John and E. L. Schwartz, unpublished data, cited in (*2*).
67. J. H. Friedman and J. M. Tukey, *IEEE Trans. Comput.* **C-23**, 881 (1974).
68. H. Zahn, *ibid.* **C-20**, 68 (1971).
69. E. R. John, P. Easton, H. Ahn, T. Harmony, P. Valdes, unpublished data cited in (*2*).
70. A. M. Starr and D. Regan, in *Proceedings of the NIMH Conference on Event-Related Potentials in Man*, Airlie House, Va., April 1977 (Academic Press, New York, in press).
71. I. M. Gerson, E. R. John, V. Koenig, F. Bartlett, *Clin. EEG* **7**, 77 (1976).
72. Weiss Institution of the Philadelphia Geriatric Center, under direction of one of us (I.G.) and V. Koenig.
73. P. Lachenbruch and M. R. Mickey, *Technometrics* **10**, 1 (1968).
74. These senile patients were evaluated psychiatrically and psychometrically in the Department of Psychiatry at New York University Medical Center by S. Gershon and S. Ferris.
75. *Wechsler Intelligence Scale for Children (WISC), Wide Range Achievement Tests (WRAT), Peabody Picture Vocabulary Test (PPVT), McCarthy Scales, Illinois Test of Psycholinguistic Abilities (ITPA)*, and the *Bender Gestalt Test* (Koppitz scoring method).
76. E. R. John, B. Z. Karmel, L. Prichep, H. Ahn, P. Easton, D. Brown, A. Toro, unpublished data cited in (*2*).
77. E. R. John and L. S. Prichep, in *Fourth International Conference on Event Related Potentials* (Hendersonville, N.C., 1976); B. Z. Karmel, H. Kaye, E. R. John, in *The XII Minnesota Symposium on Child Development* (Univ. of Minnesota Press, Minneapolis, in press).
78. P. Easton, unpublished method.
79. This study was supported by grant G 0007604516 from the Bureau of the Educationally Handicapped, Office of Education.
80. Current NB studies of normal children over a wide age range are supported by NSF/RANN grant APR 7624662.
81. H. Myklebust, in *Progress in Learning Disabilities*, M. Myklebust, Ed. (Grune & Stratton, New York, 1968), pp. 1–15.
82. H. Ahn, thesis, University of Iowa (1977).
83. This work was supported by NSF/RANN grant ERP 72-03494, formerly GI-34946, and a grant from Sandoz, Inc. B.Z.K. was supported by fellowship 1F32NS5235 from NINDS; W.C.C. was supported by Canada Council Leave Fellowship. We thank W. Torres, director of Centro Nacional de Investigaciones Cientificas de la Universidad de la Habana, for facilitating the collaboration with T.H. and P.V.; M. Lobel for her assistance; and G. Chaikin for the preparation of the computer graphics. Most of this work was carried out at the Brain Research Laboratories of the Department of Psychiatry at New York Medical College.

Natural Product Synthesis and Vitamin B_{12}

Total synthesis of vitamin B_{12} provided a framework for exploration in several areas of organic chemistry.

Albert Eschenmoser and Claude E. Wintner

Through the combined efforts of two groups, a 12-year period of research in organic natural product synthesis came to an end in 1972 with the completion of two total syntheses of cobyric acid and, hence, of vitamin B_{12}. The work was accomplished through the close collaboration of R. B. Woodward's group at Harvard and the group at the Eidgenössische Technische Hochschule (ETH). In addition to a series of published lectures (*1–3*) describing the syntheses, a lecture dealing with trends and objectives in natural products chemistry as seen from the vantage point of B_{12} synthesis has appeared in German (*4*). This article is a translated and modified version of that lecture and, in addition, includes the full scheme of the photochemical variant of the cobyric acid synthesis.

On the Role of Natural Product Synthesis

Research on the synthesis of natural products is part of the foundation of our knowledge about structure and reactivity in organic chemistry. To a large degree, our ability to prepare organic compounds, whether naturally occurring or not, has grown out of such research. The importance placed on the technological aspect of natural product synthesis has not changed substantially since the era of Adolf von Baeyer. On the other hand, its scientific function within organic and biological chemistry has altered considerably with the passage of time.

During the classical period of natural products chemistry, synthesis was an essential part of the process of structure determination. Von Baeyer's labors on indigo and Hans Fischer's on the porphyrins may stand as consummate examples. The potential ambiguity of degradative evidence made the complementary information of synthesis imperative. This classical summons of synthesis to the determination of constitution did come about, however, not because at that time there existed any greater certainty about the structural course of synthetic reactions than of degradative ones. Rather, it was the extremely high improbability that reciprocally compensating errors of interpretation would occur, which conferred the weight of proof of constitution on an identity of constitutional hypotheses derived from both degradation and synthesis. However, the development of organic natural products chemistry is characterized by the fact that the determination of constitution through chemical degradation, in principle stochastic in its methodology, yielded results far more swiftly than could the methods of synthesis, which, having specific targets, were consequently far more demanding. As the rapidly increasing number and accompanying complexity of constitutional hypotheses from degradation outstripped the possibilities of synthesis, the demand for final proof of constitution through synthesis could be satisfied in simple cases only, and then often merely in the limited form of a partial synthesis.

The gap between structure determina-

Dr. Eschenmoser is professor of organic chemistry at the Eidgenössische Technische Hochschule, CH-8092 Zürich, Switzerland. Dr. Wintner is professor of chemistry at Haverford College, Haverford, Pennsylvania 19041, on sabbatical leave at the ETH, 1976–1977.